EFFECT OF DIFFERENT REFLUX DURATIONS TOWARDS THE PHYSICAL AND CHEMICAL PROPERTIES OF VANADIUM PHOSPHORUS OXIDE CATALYSTS

CHEN JIAN JIE

A project report submitted in partial fulfilment of the
requirements for the award of the degree of
Bachelor of Engineering (Hons.) Chemical Engineering

Faculty of Engineering and Science
Universiti Tunku Abdul Rahman

May 2011

DECLARATION

I hereby declare that this project report is based on my original work except for citations and quotations which have been duly acknowledged. I also declare that it has not been previously and concurrently submitted for any other degree or award at UTAR or other institutions.

Signature : __________________________

Name : _______Chen Jian Jie______

ID No. : _______07UEB05234_______

Date : _______15th April 2011______

APPROVAL FOR SUBMISSION

I certify that this project report entitled **"EFFECT OF DIFFERENT REFLUX DURATIONS TOWARDS THE PHYSICAL AND CHEMICAL PROPERTIES OF VANADIUM PHOSPHORUS OXIDE CATALYSTS"** was prepared by **CHEN JIAN JIE** has met the required standard for submission in partial fulfilment of the requirements for the award of Bachelor of Engineering (Hons.) Chemical Engineering at Universiti Tunku Abdul Rahman.

Approved by,

Signature : _______________________

Supervisor : Dr. Leong Loong Kong

Date : _______________________

Specially dedicated to
my beloved grandmother, mother and father, elder brother, and younger sister

ACKNOWLEDGEMENTS

I would like to thank everyone who had contributed to the successful completion of this project. I would like to express my deepest gratitude to my research supervisor, Prof. Dr. Leong Loong Kong for his invaluable advice, guidance and his enormous patience throughout the development of the research.

In addition, I would also like to express my deepest gratitude to my loving parent, siblings, seniors and friends who had helped and given me encouragement on the accomplishment of the research project.

EFFECT OF DIFFERENT REFLUX DURATIONS TOWARDS THE PHYSICAL AND CHEMICAL PROPERTIES OF VANADIUM PHOSPHORUS OXIDE CATALYSTS

ABSTRACT

The vanadyl hydrogen phosphate sesquihydrate is the precursor for vanadium phosphorus oxide catalysts which is in whitish-blue powder form. It had been synthesized by refluxing vanadyl phosphate dihydrate ($VOPO_4 \cdot 2H_2O$) with 1-butanol for different lengths of time namely; 24, 48, 72 and 96 h. The catalysts that were prepared by different reflux durations had been designated as VPO-24H, VPO-48H, VPO-72H and VPO-96H. Increasing the duration of reflux led to an increase in the specific surface area from 6.77 m^2g^{-1} (VPO-24H) to 9.75 m^2g^{-1} (VPO-72H) and decreased again to 7.67 m^2g^{-1} (VPO-96H). The average V valence state for the catalysts that are determined through redox titration also increased from 4.16 (VPO-24H) to 4.25 (VPO-72H) and decreased again to 4.23 (VPO-96H). This showed that VPO-72H catalyst has the highest content of V^{5+} phase (25%). The P/V ratios obtained from ICP-OES test increased from 1.30 (VPO-24H) to 1.68 (VPO-72H) and dropped again to 1.53 (VPO-96H). For the P/V ratios obtained from the EDX test, it had the similar trend as that of ICP-OES which also increased at the beginning from 1.16 (VPO-24H) to 1.40 (VPO-72H) and then decreased to 1.28 (VPO-96H). Scanning electron microscopy showed that longer duration of reflux produced catalysts with clearer and increasing amounts of characteristic rosebud-shape agglomerates. VPO-72H appeared to have the most prominent rosebud-shape agglomerates. The analyses revealed that the VPO-72H catalyst synthesized via sesquihydrate route gives the optimal catalytic performance which is proven by the highest percentage of V^{5+} (high selectivity) and the highest P/V atomic ratio (high activity).

TABLE OF CONTENTS

CHAPTER

1 INTRODUCTION

2 LITERATURE REVIEW

3 MATERIALS AND METHODS

4 RESULTS AND DISCUSSIONS

LIST OF TABLES

LIST OF FIGURES

LIST OF SYMBOLS / ABBREVIATIONS

θ_{hkl}	diffraction angle, ° for (*h k l*) plane.
λ	X-ray wavelength of radiation for CuK_α
CuK_α	copper-alpha-potassium
β_{hkl}	full-width at half maximum (FWHM)
CO	carbon monoxide
CO_2	carbon dioxide
O	oxygen atom
VPO-24H	VPO catalyst for the reflux duration of 24 hours.
VPO-48H	VPO catalyst for the reflux duration of 48 hours.
VPO-72H	VPO catalyst for the reflux duration of 72 hours.
VPO-96H	VPO catalyst for the reflux duration of 96 hours.

LIST OF APPENDICES

CHAPTER 1

INTRODUCTION

1.1 Catalysis and Catalysts:

The term “catalysis” was first proposed by Baron J.J. Berzelius in 1835 to characterize the property of substances that facilitate chemical reactions without altering the equilibrium of the reactions. Hence, catalysis is also known as the occurrence, study, and use of catalysts in catalytic chemical reactions (M.E. Davis, 2003).

A catalyst is a chemical substance that accelerates the rate of a chemical reaction until approaching equilibrium by reducing the activation energy required for the reaction without involving itself permanently in the reaction. It is because the chemical reaction rate increases exponentially with decreasing activation energy. The role of catalyst in lowering the activation energy is by providing sites on its surface for adsorption and dissociation of the reactants where they are reacted into a product. The product then detaches from the catalyst surface and leaves it unaltered such that it is available for the next reaction (B. Viswanathan *et al.*, 2002).

Nevertheless, the catalyst does not change both the enthalpy and free energy of the reaction therefore the catalyst does not affect the equilibrium constant of the reaction. In other words, the catalyst could only increase the reaction rate until approaching to the equilibrium state but it cannot promote the occurrence of thermodynamically unfavourable reaction. This indicates that a catalyst changes only the kinetics but not the thermodynamics of a chemical reaction. The catalyst can also be added to the reactants in precursor form, which must be activated into active phase before it is used in the reaction (Chorkendorff and Niemantsverdriet, 2003).

1.2 Types of Catalysis:

There are plenty of catalysts known today in which they can be classified according to properties like; molecular structure, composition, and state of segregation. However, the state of segregation is commonly used to classify the catalysts, which is also the way they act with the reactants. There are generally two known groups of catalyst namely; heterogeneous catalysts and homogeneous catalysts

1.2.1 Homogeneous Catalysis:

It is the type of catalysts used in homogeneous catalytic processes. In homogeneous catalysis, the reactants are usually in gas-solution equilibrium. This means the catalyst and the reactants are in solution where the entire catalytic reaction takes place in the liquid phase. (M.E. Davis, 2003)

One of the common examples is the decomposition of ozone in the atmosphere via a reaction with chlorine atoms:

$$\mathrm{Cl} + \mathrm{O_3} \rightarrow \mathrm{ClO_3}$$

$$\mathrm{ClO_3} \rightarrow \mathrm{ClO} + \mathrm{O_2}$$

$$\mathrm{ClO} + \mathrm{O} \rightarrow \mathrm{Cl} + \mathrm{O_2}$$

or overall;

$$\mathrm{O_3} + \mathrm{O} \rightarrow 2\mathrm{O_2}$$

Ozone can decompose spontaneously, and also under the influence of light. However, a Cl atom acts as catalyst to accelerate the reaction. It then leaves the reaction cycle unaltered after the reaction. Since both the reactant $\mathrm{O_3}$ and the catalyst Cl are both in the same phase, namely the gas phase, the reaction cycle is an example of homogeneous catalysis (Chorkendorff and Niemantsverdriet, 2003).

In homogeneous catalysis, it normally involves metallic complexes as the catalysts (in more specific term, organometallic). Ligand effect is one of the important characteristics resulted from the metal complexes where a metal can from various products from a single substrate by just changing the ligands around the metal. One of the examples of this reaction is the catalytic carbonylation of methanol to acetic acid by$[\mathrm{Rh(CO)_2I_2}]^-$ complexes in solution;

$$\mathrm{CH_3OH + CO \rightarrow CH_3COOH}$$

Industries like pharmaceuticals production, organometallic complexes are synthesized in procedures employing molecular control in which the selection of ligands directs the reactant molecules to the desired products (Chorkendorff and Niemantsverdriet, 2003).

1.2.2 Heterogeneous Catalysis:

Heterogeneous catalysis is distinguished from the homogeneous catalysis by the different in phases present in a chemical reaction. Heterogeneous catalysis takes place between several phases where the catalyst usually is a solid, and the reactants are in either gas or liquid phase (M. E. Davis, 2003).

As solids, unless they are porous, otherwise they are commonly impenetrable. Hence, in this type of catalytic reactions, reactants normally adsorb onto the surface of a solid catalyst. The reactants are then activated by chemical interaction with the catalyst surface and transformed into adsorbed products. At the moment where the product is desorbed from the catalyst surface, the catalyst then returns to its original state and available for next reaction (B. Viswanathan *et al.*, 2002).

One of the introductory examples is the catalytic oxidation of CO on the surface of noble metals like platinum. The reaction begins with the adsorption of CO and O_2 on the surface of platinum. Then the O_2 molecule dissociates into two O atoms;

$$\mathrm{O_2} + 2^* \rightleftharpoons 2\mathrm{O}^*$$

$$\mathrm{CO} + * \rightleftharpoons \mathrm{CO}^*$$

(Note: X^* indicates that the atom or molecule is adsorbed on the surface where * is the active site on the catalyst surface). The adsorbed O atom and the adsorbed CO molecule then react on the surface to form CO_2 which interacts weakly with the platinum surface and desorbs instantaneously;

$$CO^* + O^* \rightleftharpoons CO_2 + 2^*$$

However, to maximize the reaction rates on the heterogeneous catalyst, it is important to increase the accessibility of all reactants to the active catalytic sites. The active sites are sometimes dispersed throughout the internal structure of the catalyst. For instance, a conversion of reactant A into product B at optimal rate involves the following mechanism;

i. The mass transfer or bulk diffusion (from bulk fluid) of the reactant A through the boundary layer surrounding the catalyst particle to the external catalyst surface.
ii. Diffusion of reactant A through the pore mouth of the catalyst to the catalytic surface.
iii. Adsorption of A onto the catalyst surface.
iv. Reaction of A to product B on catalytic sites on the catalyst surface.
v. Desorption of the product B molecules from the surface.
vi. Diffusion of product B through the porous network to the pore mouth.
vii. The mass transfer or bulk diffusion of the product B from the external catalyst surface to the bulk fluid.

These interactions provide an alternative path in which the formation of products from the reactants is more rapid and at milder conditions than no surface interactions. (H. S. Fogler, 2008)

1.3 Energy Profile of Reaction with Catalysts:

In a chemical reaction with the presence of catalyst, the activation energy barrier of the reaction is lowered by the catalyst through providing a surface or sites for adsorption of the reactants, formation of product and desorption of the product from the catalyst surface, in which the reactants are more readily transformed into products (Chorkendorff and Niemantsverdriet, 2003).

The energy difference between reactants and products is the heat of reaction or change in enthalpy which is positive if the reaction is exothermic. However, it is important to realize that both the enthalpy and Gibbs free energy of the catalytic reaction are unaltered by the presence of catalyst. This means that the catalyst cannot cause a thermodynamically unfavourable reaction to occur but it is able to increase the rate of reaction approaching the equilibrium state (Chorkendorff and Niemantsverdriet, 2003).

The reaction rate is a function of both temperature and reactant concentration. It is generally represented by a rate law:

$$r = k(T)C$$

where k(T) is the rate constant described by Arrhenius equation;

$$k(T) = Ae^{-E_{act}/RT}$$

Where; A is the frequency factor; R is the gas constant; T is the reaction temperature and E_{act} is the activation energy required in the reaction. The frequency factor, A is a parameter which is proportional to the number of collisions of reactant molecules which lead to the occurrence of a reaction. It is always dependent on the concentration of catalytic sites on the catalyst surfaces during a catalytic reaction. The quantity $e^{-E_{act}/RT}$ is the fraction of collisions which results in occurrence of the reaction (Bartholomew and Farrauto, 2005).

A catalyst with high concentration of active catalytic sites increases the reaction rate as well as the rate constant by increasing the frequency factor, A. Meanwhile, the activation energy, E_{act} is decreased which in turn increases the number of collisions of reactants that leads to the reaction. The activation energy is a quantity which expressing the dependency of a rate constant, k on the reaction temperature. It is also represented by the Arrhenius equation as shown above. In other words, the rate of a reaction is inversely proportional to the activation energy of the reaction. Hence, by adding catalyst to the reaction the activation energy could be lowered, then more successful collisions between molecules to occur which results in higher reaction rate (Bartholomew and Farrauto, 2005).

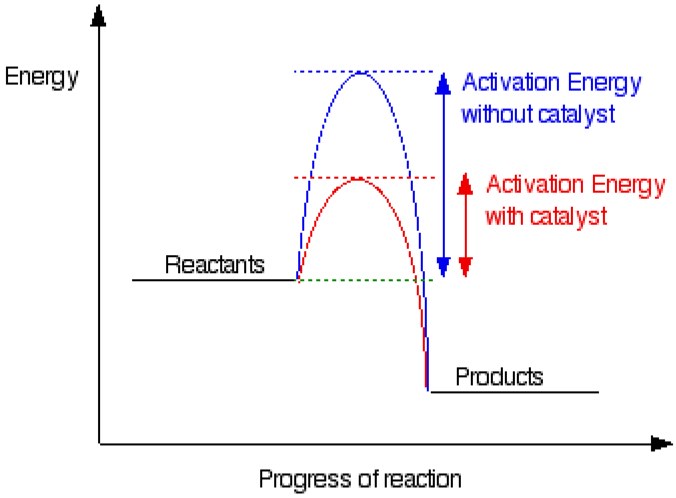

Figure 1.0: The Energy Profiles of Catalytic and Non-catalytic Reactions.

1.4 Essential Properties of Good Catalysts

Catalytic properties can be classified into dynamic, chemical and physical properties. Dynamic properties describe catalyst behaviours during catalytic reaction which include activity and selectivity. Chemical properties of catalysts include acidity, composition, oxidation state of the catalytic phase and structure. Whereas physical properties include particle size, density, pore volume, porosity, pore size and pore distribution (Bartholomew and Farrauto, 2005).

Hence, all the catalytic properties have to be optimized in order to produce a good catalyst. For instance, activity of a catalyst is increased by increasing the porosity which helps improve access to reactants and surface area of a catalyst which increases available area for a reaction. However, the optimization of chemical, physical and dynamic properties of a catalyst requires a careful selection of the component materials like active phase, promoter, and support. Other than that, catalyst morphology and geometry is another determining factor which alter the activity and selectivity of the catalyst. As an example, the surface area of a catalyst which can be increased to maximize the access of the reactant fluid to the active catalytic phase as well as to minimize the fouling of the active phase (Bartholomew and Farrauto, 2005).

Since a catalytic reaction usually occurs at the fluid-solid interface, large interfacial area essential in maximizing a reaction rate. In most of the catalysts, the large area is provided by inner porous structure. This kind of catalyst that has large area resulting from pores is called porous catalyst. However, some catalysts are sufficiently active until the porosity is not needed to boost their activity. This type of catalysts is named monolithic catalyst where pressure drop and heat removal are the major parameters to control their activity (H. S. Fogler, 2008).

Furthermore, there is another essential factor which is of utmost importance to determine the quality of catalysts which is adsorption. For a catalytic reaction to take place, at least one of the reactants or all reactants must be adsorbed onto the catalyst surface. Two different sorption processes usually occur in a catalytic reaction are; physisorption and chemisorption. For physisorption, it is relatively weak, nonselective condensation of gaseous molecules on a solid catalyst at relatively low temperatures. The attractive forces between adsorbate and adsorbent involve Van der Waals forces. Instead, chemisorption is a relatively strong and selective adsorption of chemically reactive gases on available sites of the metal surfaces at higher temperatures. The interaction normally involves formation of chemical bonds (Bartholomew and Farrauto, 2005).

1.5 Importance and Uses of Catalysts.

Catalyst has played an increasingly important role in the global chemical industry of the 20th century. Since the productivity of nearly all the chemical processes is dependent on the rate of the reactions. Nevertheless, a non-catalytic, stoichiometric reaction is generally controlled on the basis of temperature, concentration, pressure and contact time. (J.H. Clark, 2001)

Thus, by raising the temperature and pressure will enable the stoichiometric reaction to proceed at a reasonable rate of production, but the reactors in which such conditions can be safely maintained become progressively more expensive and difficult in term of fabrication. Besides, there are always thermodynamic limitations to the conditions under which products can be formed, for instance, the conversion of N_2 and H_2 into ammonia is practically impossible above 873 K. However, higher temperatures are needed to break the very strong N-N bond in N_2. Without catalysts, many reactions that are common in the chemical industry could be impossible, impractical and not economical (Chorkendorff and Niemantsverdriet, 2003).

Catalysts accelerate reactions by orders of magnitude, which enables them to be carried out under the most favourable thermodynamic conditions with much lower temperatures and pressures. Hence, catalyst technology, in combination with optimized reactor and total plant design are the key factors in minimizing both the investment and operation costs of a chemical process. (Chorkendorff and Niemantsverdriet, 2003)

1.6 Problem Statement

Maleic anhydride (MA) was first commercially produced in the early 1930s by the vapour-phase oxidation of benzene. Although benzene could be easily oxidized to MA with high selectivity, it is an inefficient raw material due to the presence of two excess atoms compared to C_4 molecule.

The production method had been dominating the global market well until 1980s. Rapid increases in the price of benzene and the recognition of benzene as hazardous raw material had become the factors that led to the first commercial production of MA from butane in 1974. Since the early 1980s, the *n*-butane-MA conversion became increasingly important and appeared as substitute to benzene-MA conversion in most of the chemical plants. Nevertheless, limited understanding on the selective oxidation of *n*-butane and the complexity of the reaction had raised concerns on the feasibility of this reaction to replace the benzene-MA conversion reaction. Hence, it is important to have an insight into the characterization and catalytic properties of the catalysts used in the selective oxidation of *n*-butane to MA which includes the selectivity and activity of the catalysts.

1.7 Objectives of Research

The main objectives of the study are to investigate the effect of reflux durations towards the physical and chemical properties of VPO catalysts and to synthesize the VPO catalysts via sesquihydrate precursor route.

CHAPTER 2

LITERATURE REVIEW

2.1 Vanadyl Pyrophosphate Catalyst $(VO)_2P_2O_7$

The selective oxidation of *n*-butane to maleic anhydride (MA) on the vanadium phosphorus oxide (VPO) catalyst is a heterogeneous gas-solid catalytic process. However, the most active phase of VPO is identified as vanadyl pyrophosphate $(VO)_2P_2O_7$ which is also one of the V^{4+} compounds, whereas the selectivity to MA is attributed to the presence of limited and controlled amount of V^{5+} sites (Bartholomew and Farrauto, 2005).

$(VO)_2P_2O_7$ molecule consists of (100) layers parallel to (010) planes in which each (100) plane is composed of pairs of $(VO)O_4$ square pyramids sharing edge (the two vanadyl groups in trans position) linked by phosphate tetrahedra. Then the layers are joined by asymmetric V=O-V bonds and P-O-P bonds of P_2O_7 groups. (Thompson *et al.*, 2001). Vanadyl pyrophosphate $(VO)_2P_2O_7$ is usually prepared from the precursor, vanadyl (IV) hydrogen phosphate hemihydrates, $VOHPO_4{\cdot}0.5H_2O$. This is done through calcination which causes the loss of water and the transformation of the hemihydrate into the pyrophosphate. The precursor, hemihydrate could be prepared from the aqueous or alcoholic solutions (Bartholomew and Farrauto, 2005).

In addition, the microstructure of $(VO)_2P_2O_7$ crystallites have great influence on the catalyst's performance. Several hypotheses had been proposed regarding the surface structures leading to the active sites of VPO catalysts:

i. Coherent interfaces formed by termination of surfaces parallel to the (100) plane of $(VO)_2P_2O_7$.

ii. A mixture of crystalline $(VO)_2P_2O_7$ and an amorphous PVO phase consisting of V^{5+} ions located in the corner-shared VO_6 octahedra at the terminus between (100) and (010) planes.
iii. An oxidized surface layer of a V^{4+} phase.

However, the second hypothesis is favoured by most chemists, concluding that the interfaces formed by termination at (100) planes of $(VO)_2P_2O_7$ can readily accommodate excess phosphorus in the form of an amorphous PVO phase. The PVO phase surrounds and isolates active centre which consists of clusters of $(VO)_2P_2O_7$, thereby limits the oxidation of n-butane. Hence, the efficiency of partial oxidation of n-butane could then be increased (Bartholomew and Farrauto, 2005).

2.2 Preparation of Vanadium Phosphorus Oxide Catalyst

Vanadium phosphorus oxide (VPO) can exist in many crystalline phases, which includes V^{5+} compounds (like $VOPO_4 \cdot 2H_2O$) and V^{4+} compounds (like $(VO)_2P_2O_7$) (Bartholomew and Farrauto, 2005).

VPO is mostly used to catalyze the selective oxidation of n-butane where n-butane is used instead of benzene as the raw material for maleic anhydride production. This is mainly due to lower price and high availability of *n*-butane with low environmental impact. One of the advantages of using VPO as catalyst in the reaction is that no support is needed in the partial oxidation of *n*-butane (Bartholomew and Farrauto, 2005).

Several routes could be used to prepare the VPO catalyst, but the most favourable one involves the reaction of vanadium (V) oxide (V^{5+} compounds) and phosphoric acid to form vanadyl (IV) hydrogen phosphate hemihydrates, $VOHPO_4$ $0.5H_2O$. This material is then heated to eliminate water from the structure which is the thermal dehydration process and form vanadyl pyrophosphate, $(VO)_2P_2O_7$, the active phase of VPO catalysts. However, there are three factors that determine the catalytic performance of the VPO catalysts namely;

i. The method of $VOHPO_4 \cdot 0.5H_2O$ synthesis. These include the parameters like types and concentration of reagents, reducing agents and solvents used in the synthesis, the reduction temperature and the synthesis duration.
ii. The procedures for activation of the precursor.

These factors are important in understanding catalytic behavior of the selective oxidation of n-butane over the VPO catalysts (Bartholomew and Farrauto, 2005).

2.2.1 Preparation of VPO in Aqueous Medium

There various routes to be available to prepare the vanadyl hydrogen phosphate hemihydrate (VHP) precursor. In the aqueous route, the V^{5+} phase is reduced by $NH_2OH \cdot HCl$ or other reducing agents followed by the addition of phosphoric acid. $VOHPO_4$ $0.5H_2O$ is then recovered by either crystallization or evaporation (Benziger *et al.*, 1997).

The VHP precursors prepared in aqueous medium are generally more crystalline (as defined by XRD) than the catalysts prepared in organic medium. The reaction for the aqueous is normally as such (Benziger *et al.*, 1997); V^{5+} compounds (V_2O_5) are reduced to V^{4+} in aqueous solutions of o-phosphoric acid and followed by the evaporation of the solvent to dryness:

$$\mathrm{V_2O_5 + NH_2OH \cdot HCl + H_3PO_4 \rightarrow VOHPO_4 \cdot 0.5H_2O \xrightarrow[773K]{} (VO)_2P_2O_7}$$

2.2.2 Preparation of VPO in Organic Medium

The organic route involves the reduction of V_2O_5 by an organic solvent (an alcohol), followed by the reaction with phosphoric acid and recovery of the solid. After recovery of VHP precursor, it is washed to remove trace amounts of water-soluble V^{5+} phase. It is then calcined at 773K, followed by final activation in air or *n*-butane / air at 673K (Benziger *et al.*, 1997).

The organic synthesis route results in platelet crystalline morphology. The size of the platelets and the way they pack are determined by the choice of organic solvent. For instance, isobutanol produces rosebud-shape morphology where the platelets agglomerate. Large alcohols such as, benzyl alcohol, appear to produce platelets with stacking faults which can be deduced from the broadening of the (200) reflection in XRD. The reaction of organic synthesis of VPO is shown as below (Benziger *et al.*, 1997):

$$\mathrm{V_2O_5 + H_3PO_4 + isobutanol \rightarrow VOHPO_4 \cdot 0.5H_2O \xrightarrow[773K]{} (VO)_2P_2O_7}$$

2.2.3 Dihydrate Precursor Route

The catalytic performance of vanadium phosphates (VPO) depends on the method of preparation of the catalyst precursor, $VOHPO_4$ $0.5H_2O$ and the reaction conditions for the activation in *n*-butane/air to form the final catalyst (Guliants and Carreon, 2005).

The active catalyst comprises $(VO)_2P_2O_7$ in combination with some V^{5+} phosphates, the transformation of the precursor to the final catalyst is topotactic. Hence, the precursor morphology is important in determining the final catalyst morphology and its performance following activation. Generally, V_2O_5 is used as a source of vanadium, and H_3PO_4 is used as a source of phosphorus. Hence, a reducing agent is required to synthesise the V^{4+} precursor phase. However, an active catalyst, can be prepared using a two-stage method based on $VOPO_4 \cdot 2H_2O$ precursor (Guliants and Carreon, 2005).

2.2.4 Hemihydrate Precursor Route

Vanadyl (IV) hydrogen phosphate hemihydrate, $VOHPO_4$ $0.5H_2O$ is the common precursor of the VPO catalysts for the selective oxidation of *n*-butane to maleic anhydride (Guliants and Carreon, 2005).

The hemihydrate is usually prepared by refluxing its component oxides in alcohol. Vanadyl pyrophosphate $(VO)_2P_2O_7$, the active phase of VPO catalysts is usually obtained by the thermal treatment of the hemihydrate precursor in a mixture of *n*-butane in air. However to obtain optimal VPO catalysts, the following synthesis conditions of hemihydrates precursor are necessary;

i. Synthesis of microcrystalline $VOHPO_4.0.5H_2O$ in an alcohol characterized by the exposure of the basal (001) planes.
ii. Presence of defects in the stacking of the (001) planes.
iii. Excess of phosphate with respect to the stoichiometric amount applied in the synthesis with P/V ratio at 1.01-1.10. The excess phosphate is strongly bound to the surface and cannot be removed by simple washing of the precursor in polar solvents.

(Guliants and Carreon, 2005)

There are commonly three major synthesis methods were reported for preparation of the $VOHPO_4.0.5H_2O$ precursor:

i. In aqueous synthesis, V^{5+} compounds (V_2O_5) are reduced to V^{4+} in aqueous solutions of o-phosphoric acid and followed by the evaporation of the solvent to dryness;

$$V_2O_5 + 2NH_2OH - HCI + 2H_3PO_4 \rightarrow 2VOHPO_4.0.5H_2O + N_2 + 2HCl + 4H_2O$$

ii. In organic synthesis, V^{5+} compounds are reduced by an anhydrous alcohol, followed by the addition of anhydrous o-phosphoric acid dissolved in the same alcohol with the precipitation of $VOHPO_4 \cdot 0.5H_2O$:

$$V_2O_5 + EtCHOMe + 2H_3PO_4 \rightarrow 2VOHPO_4 \cdot 0.5H_2O + EtCOMe + 2H_2O$$

iii. In model organic synthesis, V^{5+} o-phosphate dihydrate, $VOPO_4 \cdot 2H_2O$ is first synthesized from V_2O_5 and H_3PO_4 in aqueous medium and then only reduced to $VOHPO_4\ 0.5H_2O$ by an alcohol in a separate step;

$$V_2O_5 + 2H_3PO_4 + H_2O \rightarrow 2VOPO_4 \cdot 2H_2O + H_2O$$

$$2VOPO_4 \cdot 2H_2O + EtCHOHMe \rightarrow 2VOHPO_4 \cdot 0.5H_2O + EtCOMe + 3H_2O$$

Normally the organic synthesis provides the most active and selective catalysts. However, all three methods may also lead to various hydrated vanadyl (IV) hydrogen phosphate phases, $VOHPO_4 \cdot nH_2O$ (n = 0.5,1,2,3, and 4)**,** which are all precursors of the VPO catalysts. Nevertheless, the precursor with n = 0.5 ($VOHPO_4.0.5H_2O$) produces the best VPO catalysts. (Guliants and Carreon, 2005).

2.2.5 Sesquihydrate Precursor Route

Vanadyl hydrogenphosphate sesquihydrate ($VOHPO_4 \cdot 1.5H_2O$) is recently developed and alternative route in producing vanadyl pyrophosphate, $(VO)_2P_2O_7$.

It is prepared by reduction of $VOPO_4 \cdot 2H_2O$ suspended in refluxed 1-butanol and activated at 753 K over 10 hours on-stream to form vanadyl pyrophosphate, $(VO)_2P_2O_7$. It revealed high specific activity per unit surface area in the vapour-phase oxidation of *n*-butane. By employing 1-butanol as solvent, the sesquihydrate could be intercalated with cobaltous acetate to afford modified $(VO)_2P_2O_7$ with high activity. However, both selectivity to maleic anhydride and surface area decreases with increasing cobalt contents. (Taufiq Yap *et al.*, 2004)

2.3 Parameter of Vanadium Phosphorus Oxide Catalyst (VPO)

The activity and selectivity of VPO catalyst in the selective oxidation of n-butane to maleic anhydride could be attributed to several essential parameters namely; calcinations of the VPO catalyst precursor, selection of catalyst support material, dopants (promoters) added to the catalyst and the P/V atomic ratio of the VPO catalyst. All these parameters are the key factors that could be altered and controlled in order to optimize the performance of VPO catalyst in the oxidation process.

2.3.1 Parameter: Calcination Condition

Calcination is a high-temperature treatment of catalyst precursors in air which is usually the final step in producing oxide catalysts or the second-last step in producing metal catalysts. The main purpose of carrying out calcination is to decompose and volatilize various volatile impurities or catalyst precursors formed during the preparation process. They are normally not the desired forms for the final catalysts like hydroxides, nitrates and carbonates (Bartholomew and Farrauto, 2005).

For the decomposition of unsupported hydroxide or carbonate precursors, or precursors supported on inorganic oxide carriers, calcinations is normally conducted at air temperatures between 300℃ and 500℃. However, the solids must be pre-dried carefully and to avoid rapid heat-up during calcination. This is because H_2O trapped in the micropores can build up pressure which is sufficient to crack the particulate supports. Moreover, exothermic reactions due to the decomposing salts can cause localized high temperatures within the catalyst material. This will then lead to sintering of the supports and catalysts (Bartholomew and Farrauto, 2005).

In the preparation of VPO catalysts, the well-crystallized active phase of VPO catalysts for synthesis of MA, vanadyl pyrophosphate $(VO)_2P_2O_7$ is generally generated by a long-term calcination of the precursor, $VOHPO_4 \cdot 0.5H_2O$ prepared via reduction of $VOPO_4 \cdot 2H_2O$ using isobutanol as reducing agent followed by treatment in a reaction environment. Transformation of precursor to active phase and the surface properties of the active VPO can be affected by the temperature, time and atmosphere of calcination (Taufiq-Yap and Saw, 2007).

2.3.2 Parameter: Support System

Small metal catalyst particles are often unstable and tend to sinter at the temperatures of catalytic reactions. Thus, particularly for heterogeneous catalysis, these small metal particles are prevented from sintering by applying the particles inside the pores of an inert catalyst support which is usually less active than the catalyst particles (Bartholomew and Farrauto, 2005).

Catalyst supports are normally porous metal oxides which have high surface area or carbons that have significant pore volume and capacity for preparing and preserving stable, well-dispersed catalytic phases during catalytic reaction. Among all, alumina, silica and carbon are the most common with magnesia, titania, zirconia, zinc oxide, silicon carbide and zeolites used for particular applications. They are commonly used in the industrial catalytic processes because of their excellent thermal stability and the wide range of chemical, physical and some other catalytic properties (Bartholomew and Farrauto, 2005).

However, for the supported VPO catalysts, they usually consist of V^{5+} phases, mostly in α-$VOPO_4$ or γ-$VOPO_4$ form, and exhibit low MA selectivity as well as low *n*-butane conversion. Other than that, some supported VPO catalysts exhibit interesting behaviours. For example, titania-supported VPO is active even at moderate temperatures like 523 K. This is due to the strong interaction between the

VPO and the reducible support titania. This then causes the VPO to be more reducible and enhances the catalytic activity, but the MA selectivity is still relatively low (Ruitenbeek *et al.*, 1998). Nevertheless, for the silica-supported VPO catalyst, it improves the MA selectivity in the expense of *n*-butane conversion (Nie *et al.*, 2002).

2.3.3 Parameter: Doped System

Dopant is an active ingredient which is usually added to catalysts in small amounts during a catalytic reaction to increase their activity. This substance is also called promoter (Bartholomew and Farrauto, 2005).

Promoters are classified into two types namely; textural and chemical. Textural promoters are generally used to facilitate the preparation of well-dispersed catalytic phases as well as to maintain the well-dispersed state during the catalytic reaction. Textural promoters include the catalyst supports such as alumina, silica and other inert oxides with high surface area that serve the above two purposes. For chemical promoters, they are additives that added to catalysts during a reaction to enhance the activity and selectivity of the catalysts. Typical chemical promoters include alkali earth metals or metal oxides (Bartholomew and Farrauto, 2005).

Particularly in the selective oxidation of *n*-butane to maleic anhydride over the VPO catalyst, the promoters have twofold structural role namely; to enable the formation of the required VPO compounds and decrease the formation of deleterious phases. Besides, it also enables the formation of solid solutions that regulate the catalytic activity of the solid. A wide range of cations have been added as the modifiers to catalyst with some beneficial effects. Many studies had shown the influence of the added promoters on the yield and selectivity for maleic anhydride formation as well as the reaction rate over the catalysts. (Bartholomew and Farrauto, 2005)

One of the common dopants added onto VPO catalyst during the oxidation of *n*-butane is cobalt, Co. The Co-doped VPO catalysts is prepared from the reaction of V_2O_5 and H_3PO_4 or $VOPO_4 \cdot 2H_2O$ with isobutanol. The Co addition acts as a structural promoter. The smallest amounts of dopant produced the most beneficial effect. Zazhigalov *et al.*, 1993 proposed that Co stabilizes the catalyst performance by forming cobalt phosphate, which improves its catalytic properties. Volt *et al.*, 2003 found that the incorporation of Co can modify the V^{5+}/V^{4+} balance during the activation period and also change the catalytic performance in the steady state. By NMR techniques, they observed that the presence of the Co dopant inhibits the transformation of the precursor and stabilizes an amorphous vanadium phosphate. (Corgnalia *et al.*, 2003)

2.3.4 Parameter: P/V Atomic Ratio

An optimal catalyst composition is characterized by a slight excess of phosphate with respect to the empirical formula of the $VOHPO_4 \cdot 1.5H_2O$ precursor. A considerable excess of surface phosphate (P/V = 1.5-3.0 by XPS) prevents the bulk oxidation of $(VO)_2P_2O_7$ to $VOPO_4$ phases. In catalysts with a slight phosphate deficiency (P/V = 0.95), the rates of V^{4+} oxidation and reduction are high (Cavani *et al.*, 1992). The increased V^{5+} content leads to more active but less selective catalysts, while low reducibility of V^{4+} in VPO catalysts with high surface phosphate concentration results in low catalytic activity (Guliants and Carreon, 2005).

Hence, catalysts with slight excess of phosphate (P/V = 1.05) show the right compromise between reducibility and oxidizing ability required to obtain both high activity and selectivity in *n*-butane oxidation. The excess phosphate terminates the side faces of the (200) plane $(VO)_2P_2O_7$ in the form of the surface $VO(PO_3)_2$ phase which prevents the oxidation of vanadyl pyrophosphate due to lower oxidizing ability of $VO(PO_3)_2$ (Matsuura and Yamazaki, 1990).

2.4 Maleic Anhydride

Maleic anhydride (MA) is a multifunctional chemical intermediate that has applications in nearly every field of industrial chemistry. It has the following chemical structure:

Figure 2.1: The Molecular Structure of Maleic Anhydride, $C_4H_2O_3$.

Its molecule contains two acid carbonyl groups and a double bond at α- β position. It is colourless or white solid with chemical formula $C_4H_2O_3$. According to the single crystal XRD data, the molecule of maleic anhydride is nearly planar in structure with ring oxygen atoms lying out of the molecular planar. It is an important raw material used in the manufacture of phthalic-type alkyd and unsaturated polyester resins, surface coatings, lubricant additives, copolymers and agricultural chemicals (Felthouse *et al.*, 2001).

Maleic anhydride was first synthesized in the 1830’s, but was not manufactured commercially until about 1930. Initially, it was produced through the partial oxidation of benzene using a vanadium molybdenum oxide catalyst (V_2O_5-MoO_3). This process involved the oxidation of a low concentration of benzene in air followed by a separation step to recover MA from the reactor effluent. The conversion is high (about 97-99%) and the MA selectivity is near 75% with by-products CO and CO_2 (Felthouse *et al.*, 2001).

However, benzene is a hazardous chemical. Over the years of research, n-butane is found to be a better substitute of benzene for MA production, which was first realized by Monsanto in 1974. Compared to the benzene oxidation to MA, n-butane partial oxidation to MA was more economical, safer and more environmentally benign (Chorkendoff and Niemantsverdriet, 2003).

2.4.1 Uses of Maleic Anhydride

Maleic anhydride (MA) is a versatile monomer and important chemical intermediate with many applications. The primary use of maleic anhydride is in the manufacture of polyester and alkyd resins. These resins are added to fibre-glass reinforced plastics to produce a strong, light-weight, and corrosion resistant material that is found in boats, cars, trucks, pipelines and electrical devices (Felthouse *et al.*, 2001).

It is also used as ingredient in the manufacture of lacquers, lube-oil additives, and agricultural products. The addition of MA to drying oils decreases the required drying time and improves the coating quality of lacquers; dispersants which derived from MA can prolong oil change intervals as well as to improve the efficiency of automotive engines. The use of maleic anhydride in the manufacture of agricultural chemicals is another common application. Pesticides like Malathion and Difolatan are produced by using maleic anhydride as the major ingredient (Felthouse *et al.*, 2001).

MA can also be used to produce a vinyl copolymer through the co-polymerization of MA with other molecules that contain vinyl functionality. Typical copolymers are styrene-maleic which is used to produce engineering thermoplastic, paper treatment chemical, floor polishes, adhesives, detergents (acrylic acid-maleic) and cosmetics. Moreover, there are also some further applications in which maleic anhydride serves as a raw material. These applications are based on the versatility of this molecule. One of them is the production of an artificial sweetener, aspartame. It is a dipeptide with one amino acid (L-aspartic acid) which is produced from maleic anhydride as the starting material (Felthouse *et al.*, 2001).

Furthermore, MA can also form copolymers with mono-O-methyl-oligoethylene glycol vinyl ethers that are partially esterified for biomedical and pharmaceutical uses. The recently developing use for maleic anhydride is the synthesis of 1,4-butanediol from MA. Butane is first oxidized to MA, which is recovered as maleic acid and then reduced to tetrahydrofuran. Almost half of the world production of 1,4-butanediol is dehydrated to tetrahydrofuran to make fibres like Spandex (synthetic fibre known for its exceptional elasticity) (Chorkendorff and Niemantsverdriet, 2003).

2.4.2 Oxidation of *n*-butane to Maleic Anhydride

Selective oxidation of of *n*-butane to maleic anhydride over the VPO catalysts is recognized as one of the most complex selective oxidations which involves eight H atoms abstraction and three O atoms insertion with 14 electrons transferring. It is a redox reaction in which the n-butane is partially oxidized by lattice oxygen in the feed stream (Felthouse *et al.*, 2001).

The reaction of *n*-butane to maleic anhydride (MA) is highly exothermic ($\Delta H_r = -1260 \text{ kJ/mol}$ at 700 K) and accompanied by total oxidations to COx (CO and CO_2) in addition to H_2O at 700 K. In view of the complexity of the reaction, the proposed mechanism is also very complicated and involves alternate paths. The reaction is believed to follow a Mars-van Krevelen (redox) mechanism, in which the catalyst provides lattice oxygen to oxidize the adsorbed reactants and is reduced. The consumed lattice oxygen is then replenished by the surface oxygen species converted from gaseous oxygen and the catalyst is regenerated. The mechanism consists of seven or more steps including dehydrogenation of *n*-butane to *n*-butene, isomerisation, further dehydrogenation to *n*-butadiene, addition of oxygen to a double bond, ring formation as well as further step-wise addition of two O atoms. Nevertheless, this mechanism is still arguable among researchers especially on the intermediates formation (Felthouse *et al.*, 2001).

Despite of the limited understanding on the reaction kinetics, the preparation and characterization of the VPO catalysts used for *n*-butane oxidation to MA have been intensely studied. Several routes could be applied to prepare the catalyst, but the route favoured by industry involves the reaction of vanadium (V) oxide (V^{5+} compounds) and phosphoric acid to form vanadyl hydrogen phosphate, $VOHPO_4$ $0.5H_2O$. This material is then heated to eliminate water from the structure and form vanadyl pyrophosphate, $(VO)_2P_2O_7$. Vanadyl pyrophosphate is believed to be active phase required for the conversion of *n*-butane to maleic anhydride (Felthouse *et al.*, 2001).

CHAPTER 3

MATERIALS AND METHODS

3.1 Materials and Gases used

Below are the chemicals used throughout this study:

1. Vanadium (V) pentoxide, V_2O_5 (Merck)
2. *ortho*-Phosphorus acid, *o*-H_3PO_4 (85%) (Merck)
3. 1-Butanol, $CH_3(CH_2)_3OH$ (R&M Chemicals)
4. Nitric acid, HNO_3 (R&M Chemicals)
5. Sulphuric acid, H_2SO_4 (95- 98%) (Merck)
6. Potassium permanganate, $KMnO_4$ (Fisher Scientific)
7. Ammonium iron (II) sulphate, $(NH_4)_2Fe(SO_4)_2$ (R&M Chemicals)
8. Diphenylamine, Ph_2NH (ACROS)
9. Ammonium Dihydrogen Phosphate, $NH_4H_2PO_4$ (Merck)
10. Ammonium metavanadate, NH_4VO_3 (Merck)

The gases used throughout this study:

1. 0.75 % *n*-butane in air (Malaysia Oxygen Berhad, MOX)
2. 99.99 % Purified Nitrogen (Malaysia Oxygen Berhad, MOX)
3. 99.99 % Purified Helium (Malaysia Oxygen Berhad, MOX)
4. 99.99 % Purified Argon (Malaysia Oxygen Berhad, MOX)
5. Liquefied Nitrogen Gas (Malaysia Oxygen Berhad, MOX)
6. Compressed Air (Malaysia Oxygen Berhad, MOX)

3.2 Methodology

Generally, the preparation of the bulk vanadyl pyrophosphate catalysts can take place via different routes; notably the sesquihydrate route (VPOs), the organic route (VPOo) and the reduction of Vanadyl phosphate dihydrate, $VOPO_4 \cdot 2H_2O$ phase (VPOd). The preparation of the doped vanadyl pyrophosphate catalysts can take place via organic route and the reduction of $VOPO_4 \cdot 2H_2O$ phase. In this research, the preparation of the vanadium phosphorus oxide catalyst takes place via the sesquihydrate precursor $VOHPO_4 \cdot 1.5H_2O$.

3.2.1 Preparation of the Vanadyl Phosphate Dihydrate ($VOPO_4 \cdot 2H_2O$)

The production of vanadyl pyrophosphate catalyst has been developed via vanadyl hydrogen phosphate sesquihydrate precursor, $VOHPO_4 \cdot 1.5H_2O$ [I. Matsuura, 1995]. The synthesis of sesquihydrate precursor has been divided into a two-step procedure, which involving vanadyl phosphate dihydrate, $VOPO_4 \cdot 2H_2O$ as an intermediate before obtaining the precursor.

Firstly, 15 g of vanadium pentoxide, (V_2O_5) was weighed. It was then added with 90 ml of *ortho*-phosphorus acid, *o*-H_3PO_4 (85 %) and 360 ml of distilled water. The mixture was then refluxed for 24 hours at 120 °C. A yellow intermediate will be formed. The mixture was cooled to room temperature and was centrifuged. Yellow solids recovered by centrifuge technique, were washed sparingly with acetone and were ovendried (~80 °C) for 24 hours. The yellow solids obtained are vanadyl phosphate dihydrate ($VOPO_4 \cdot 2H_2O$).

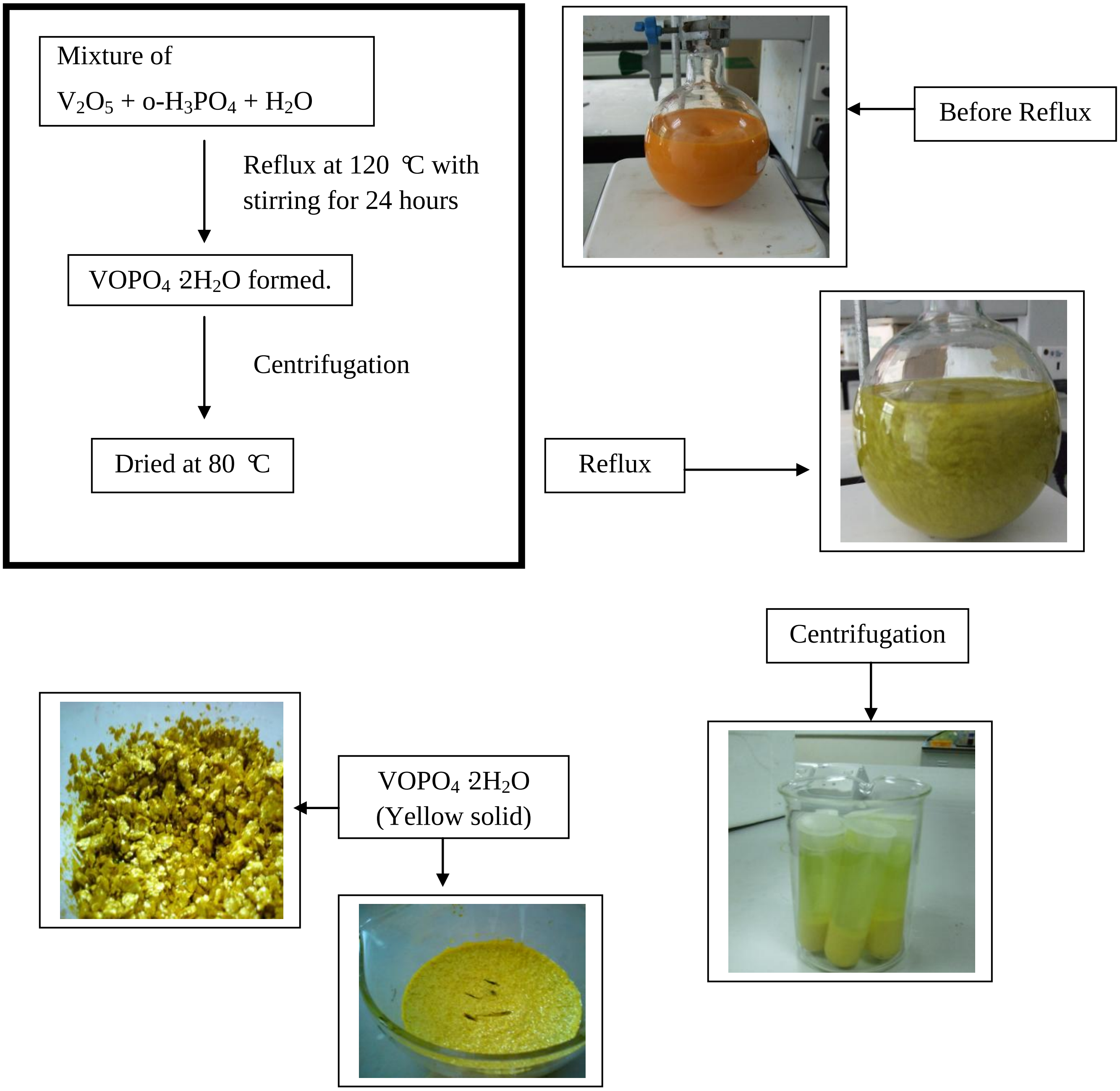

Figure 3.0: The Diagrams Show the Preparation Steps of $VOPO_4 \cdot 2H_2O$

3.2.2 Preparation of the Vanadium Phosphorus Oxide Catalysts

10 g of $VOPO_4 \cdot 2H_2O$ precursors were added with 150 ml 1-butanol. The mixture was then under reflux for 24 hour. After being cooled to room temperature, the resultant precipitate which is whitish-blue powder is referred to vanadyl hydrogen phosphate sesquihydrate precursor. Whitish-blue powder was recovered by centrifuge technique, washed sparingly with acetone and oven-dried at 80 ℃ for 24 hours. The procedure was repeated for another three sets of the precursor-alcohol mixtures in which they were refluxed for 48 hours, 72 hours and 96 hours.

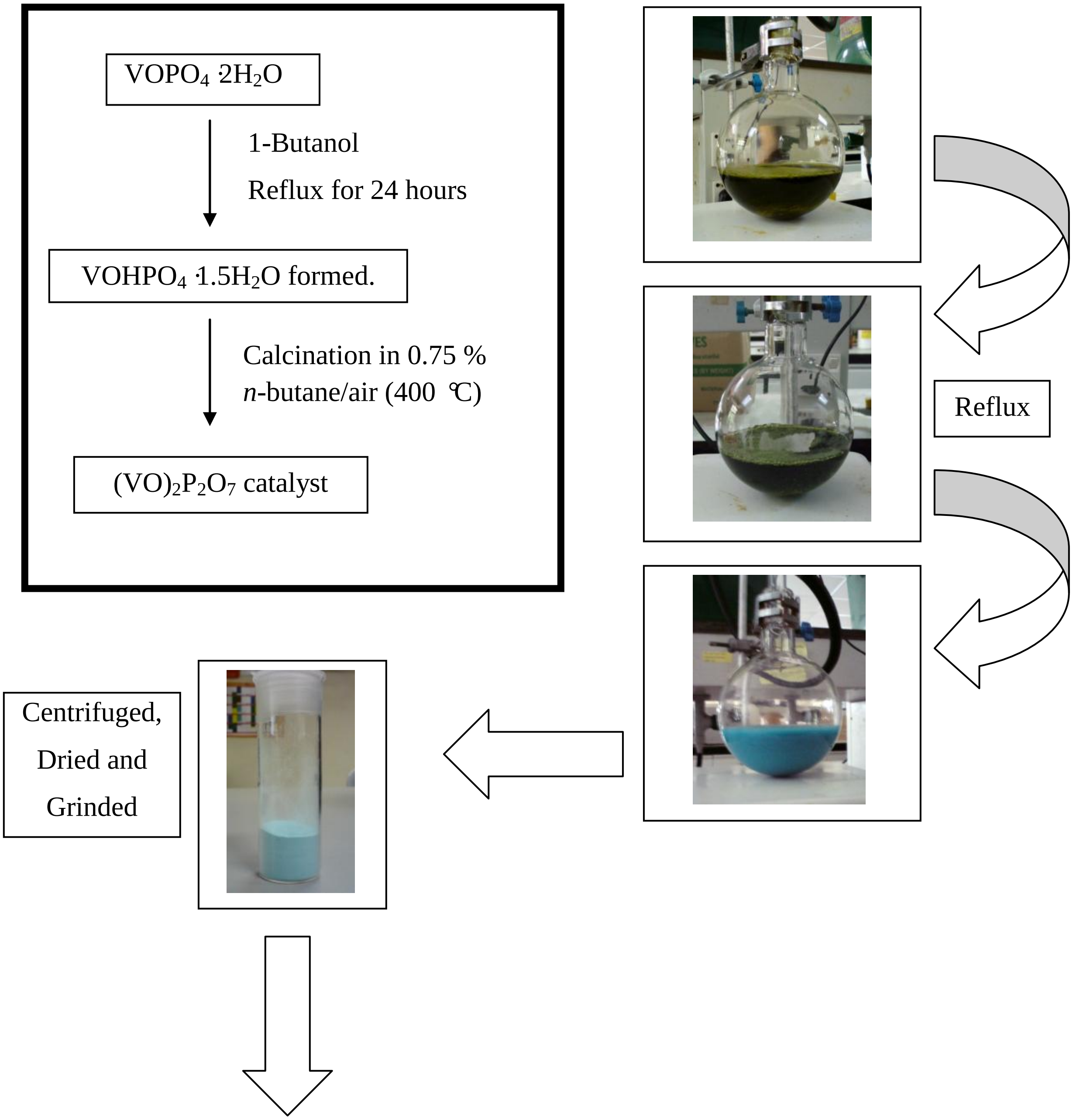

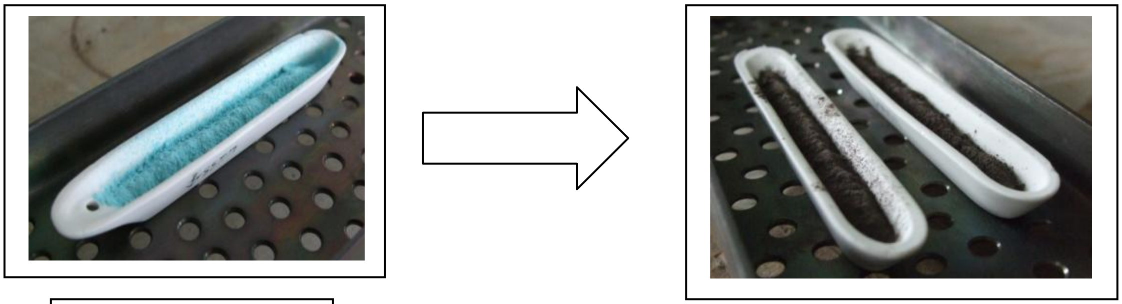

Before calcination

After calcination

Figure 3.1: The Diagrams Show the Preparation Steps of $(VO)_2P_2O_7$.

3.3 Characterisation Techniques and Instrumentations

Throughout the research, there are some instruments involved to examine the physical and chemical properties of the catalysts produced. They are used to analyse the catalyst formed, which is vanadyl pyrophosphate catalyst. The machines and techniques used are notably, X-Ray Diffractometer, BET surface area measurement, Scanning Electron Microscopy with Energy Dispersive X-Ray Spectrometer (SEM-EDX), and Redox Titration.

3.3.1 X-Ray Diffraction (XRD) Analysis

X-Ray Diffraction (XRD) analysis is a machine used to determine the phase composition of catalyst at ambient temperature and under normal atmospheric conditions. It is one of the most powerful and efficient techniques for qualitative and quantitative analysis of crystalline compounds. It relies on the dual wave or particle nature of X-Rays to obtain information about the structure of crystalline materials. The sample is prepared for analysis by packing a small amount of sample into a shallow cup. Sometimes the sample can be introduced as slurry and placed on a quartz slide.

The phenomenon of diffraction occurs when the penetrating radiation, X-rays enters a crystalline substance and is scattered. The scattered X-rays will undergo constructive and destructive interference in a process termed as diffraction. In order for a beam to be 100 % diffracted, the distance it travels between rows of atoms at the angle of incidence must be equal to an integral multiple of the wavelength of the incident beam. D-spacings which are greater or lesser than the wavelength of the directed X-ray beam at the angle of incidence will produce a diffracted beam of less than 100 % intensity. Sample will rotate during the analysis to reduce any heating to the sample. Resulting diffractogram will confirm the identity of a solid material as a pharmaceutical powder. The diffraction of X-Rays by crystals is described by Bragg's Law. X-Rays are reflected from a crystal only if the angle of incidence satisfies the condition $n\lambda = 2d \sin \theta$ (M.S. Whittingham, 1997).

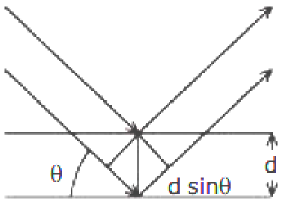

Figure 3.2: The Incident X-rays Scattered by Atoms in an Orderly Arranged Lattice Planes.

X-ray diffraction has been in use in two main areas; the fingerprint characterization of crystalline materials and the determination of their structure. Each crystalline solid has its unique characterization X-ray powder pattern which may be used as a "fingerprint" for its identification. Once the material has been identified, X-ray crystallographic may be used to determine its structure, *i.e.* how the atoms pack together in the crystalline state and what the interact-atomic distance and angle are *etc*. therefore, size and the shape of the unit cell for any compound most easily determined by using the diffraction of X-rays. In catalysis, X-ray diffraction analysis is carried out to determine the phase compositions of catalysts at ambient temperature and under normal atmospheric conditions. Therefore, the relative abundance of V^{4+} and V^{5+} can be determined. The crystallite sizes can also be determined by using Debye-Scherrer equation:

$$t = \frac{0.89\lambda}{\beta_{hkl} cos\ \theta_{hkl}}$$

Where t is the crystallite size for ($h\ k\ l$) phase, λ is the X-ray wavelength of radiation for CuKα, $\beta_{h\,k\,l}$ is the full-width at half maximum (FWHM) at ($h\ k\ l$) phase and $\theta_{h\,k\,l}$ is the diffraction angle for ($h\ k\ l$) phase (Klug and Alexander, 1974).

In this study, X-ray diffraction (XRD) patterns were obtained using a Shimadzu diffractometer model XRD-6000 employing CuKα radiation generated by a Philips glass diffraction X-ray tube broad focus 2.7 kW type on the catalysts at ambient temperature. The basal spacing was determined via powder technique. The samples were scanned at the range 2θ = 2 °-60 ° with a scanning rate of 1.2000 ° min^{-1}. The diffractograms obtained were matched against the Joint Committee on Powder Diffraction Standards (JCPDS) PDF1 database version 2.6 to confirm the catalysts phases.

Figure 3.3: Shimadzu Diffractometer Model XRD-6000

3.3.2 BET Multiple Point Surface Area Measurement

The Brunauer-Emmett-Teller (BET) analysis involves the nitrogen adsorption at low temperature has been used for the determination of the multiple point surface area of porous materials, using Thermo Finnigan Sorptometic 1990.

It is based on the multi-layer molecular adsorption model proposed by Stephen Brunauer, Paul Hugh Emmett and Edward Teller, in which single layer adsorption volume, V_m is correlated with multi-layer adsorption volume, V. The following is the famous BET equation (Beijing JWGB, 2009):

$$\frac{V}{V_m} = \frac{cx}{(1-x)[1+(c-1)x]}$$

Where;

$$x = \frac{P}{P_0}$$

P = Nitrogen partial pressure

P_0 = Nitrogen saturation vapour pressure at liquid phase nitrogen temperature

V = Real absorption volume on sample surface

V_m = Monolayer nitrogen absorption volume

c = Constant related to heat of adsorption and desorption

Since BET equation is based on multi-layer adsorption theory, which makes it more accurate to describe real adsorption process. Measurement by BET method ensures better accuracy. Through measurement of 3 to 5 groups of multi-layer adsorption volume by sample at different partial nitrogen pressure, an adsorption isotherm can be plotted with P/Von the y-axis and P/P_0 on the x-axis according to experimental results. Fit this curve to get a straight line, slope and intercept can then be obtained. Surface area of sample under testing can be calculated from known V_m. Based on theory and practice, BET equation fits well with real adsorption process when P/P_0 is in the range of 0.35-0.05 (Beijing JWGB, 2009).

The operating principle of the BET sorptometer is as following; a sample contained in an evacuated sample tube is cooled to cryogenic temperature then exposed to nitrogen gas at a series of precisely controlled pressures. With each incremental pressure increase, the number of gas molecules adsorbed on the surface increases. The pressure at which adsorption equilibrium occurs is measured and the universal gas law is applied to determine the quantity of gas adsorbed. As adsorption proceeds, the thickness of the adsorbed film increases. Any micropores in the surface are quickly filled, then the free surface becomes completely covered and finally larger pores are filled (J. Cantolina, 2010).

The process may continue to the point of bulk condensation of the nitrogen gas. After that, desorption process may begin in which pressure is reduced resulting in liberation of the adsorbed molecules. As with the adsorption process, the changing quantity of gas on the solid surface is quantified. These two sets of data describe the adsorption and desorption isotherms. Analysis of the isotherms yields information about the surface characteristics of the material (J. Cantolina, 2010).

Figure 3.4: BET Sorptometer: Thermo Finnigan Model Sorptometic 1990

3.3.3 Redox Titration

This method was developed by Miki Niwa and Yuichi Murakami in 1982. They had investigated the reaction mechanism of the ammoxidation of toluene on V_2O_5/ Al_2O_3 catalyst. The bifunctional activity of this catalyst which consists of the oxidation activity of V_2O_5 and the dehydration property of Al_2O_3 is stressed. However, some problems about the active sites of vanadium oxide and alumina and how they actually contribute to the ammoxidation of toluene remain a question. (Niwa and Mukakami, 1982).

In this research, redox titration was carried out to determine the average vanadium valance (AV) of the VPO catalysts and/ or to obtain the average oxidation state of vanadium. First, a known amount of the sample is dissolved in 100 ml sulphuric acid (2 M). it is then cooled to room temperaturue before being titrated with potassium permanganate solution (0.01 N). this titrant is used to oxidize V^{3+} and V^{4+} in the solution to V^{5+}. The end point is reached when the change of colour from the original greenish blue to pink was observed. The volume fo potassium permanganate used was recorded as V_1. Then the oxidized solution was treated with ammonium iron (II) sulphate solution (0.01 N). This is to reduce V^{5+} to V^{4+} in the solution. Diphenylamine is used as an indicator. The end point is reached when the purple colour of the solution disappeared and became colourless. The volume of ammonium iron (II) sulphate used was recorded as V_2 (Niwa and Mukakami, 1982).

Another fresh 25 ml of the original solution was then titrated with 0.01 N ammonium iron (II) sulphate solution. Diphenylamine is also used as indicator. This stage of titration is to determine the V^{5+} in the original solution. The end point is reached when the solution changes from purple to greenish blue. The volume of ammonium iron (II) sulphate solution used was recorded as V_3.

The average oxidation state of vanadium (AV) can be determined by solving the equation below:

$$AV = \frac{5V^{5+} + 4V^{4+} + 3V^{3+}}{(V^{5+} + V^{4+} + V^{3+})}$$

where V^{3+}, V^{4+} and V^{5+} are concentration of vanadium at different oxidation state. In order to obtain values for V^{3+}, V^{4+} and V^{5+} values, respectively. The following equations are used:

$$V^{3+} = 20(0.01)V_1 - 20(0.01)V_2 + 20(0.01)V_3$$

$$V^{4+} = 40(0.01)V_2 - 40(0.01)V_3 - 20(0.01)V_1$$

$$V^{5+} = 20(0.01)V_3$$

where V_1= the volume of potassium permanganate used and V_2= the volume of ammonium iron (II) sulphate used (Niwa and Mukakami, 1982).

3.3.4 Inductively Coupled Plasma-Optical Emission Spectrometer (ICP-OES)

ICP-OES is a sophisticated instrument used to detect the trace elements. Quantitative and qualitative analysis of the VPO catalysts were performed on a Perkin-Elmer Emission Spectrometer Model Plasma 1000. The molar ratios of the elements, P/V ratios were determined using this technique. The catalyst samples were digested in 10 mL of 8 M nitric acid (HNO_3) to release the metal elements into solution for analysis (Masilo, 2009).

The multi elemental standards of the elements under research were prepared in the 6.25 to 50 ppm concentration range for vanadium and phosphorus. The actual concentrations of the existing elements in the samples were determined from this range of standards using the calibration graphs obtained from the element standards. The range of elemental standards used for the analysis is given in Table 3.1 (Masilo, 2009).

Table 3.0: The range of calibration standards used in the ICP- OES

Element	**Concentration Range (ppm)**			
Vanadium, V	50.00	25.00	12.50	6.25
Phosphorus, P	50.00	25.00	12.50	6.25

In this technique, the sample is aspirated into an inductively coupled plasma discharge. The analyte is then converted into the gas-phase atoms in their excited states. Following this, the emitted light produced by the excited atoms is measured relative to the concentration range of the standards to give the sample concentration. (Masilo, 2009)

Figure 3.5: ICP-OES: Perkin-Elmer Emission Spectrometer Model Plasma 1000

3.3.5 Scanning Electron Microscopy with Energy Dispersive X-ray Spectrometer (SEM-EDX)

The scanning electron microscopy (SEM) analyses were done by using a Hitazchi S-3400N electron microscope, whereas Energy-dispersive X-ray (EDX) analyses were carried out by using EDAX software.

SEM is used for examining topographies and morphologies of specimens at very high magnification. It uses a focused scanned electron beam to produce images of the sample, both top-down and cross-sections. The primary electron beam interacts with the sample in the following ways:-

- Primary electrons generate low energy secondary electrons, which tend to emphasise the topographic nature of the specimen.
- Primary electrons can be backscattered which produces images with a high degree of atomic number contrast.
- Ionized atoms can be relaxed by electron shell-to-shell transitions which lead to either X-ray emission or Auger electron ejection. The X-rays emitted are characteristic of the elements in the top few μm of the sample and are measured by the EDX detector (LDP Lab Services, 2010).

EDX is an analytical technique, used for identifying the elemental composition of the specimen. It functions as an integrated feature with a SEM. EDX analysis is normally carried out on a thin evaporated layer on top of a nickel / iron alloy. The layer contains a mixture of barium, strontium and oxygen, with a small amount of magnesium. The thickness of the layer was calculated to be about 38 nm (K. Raper, 2010).

Figure 3.6: SEM-EDX Model Hitachi S-3400N

CHAPTER 4

RESULTS AND DISCUSSION

4.0 Introduction

The characterization of the VPO catalysts for different durations of second-stage reflux carried out through;

i. X-ray Diffraction (XRD) Technique
ii. Brunauer-Emmett-Teller (BET) Method
iii. Inductively Coupled Plasma-Optical Emission Spectrometer (ICP-OES)
iv. Redox Titration
v. Scanning Electron Microscopy (SEM) Analysis
vi. Energy-Dispersive X-ray (EDX) Analysis.

In this chapter, VPO catalysts for the reflux duration of 24, 48, 72 and 96 hours are denoted as samples; VPO-24H, VPO-48H, VPO-72H and VPO-96H respectively.

4.1 X-ray Diffraction (XRD) Analysis

The VPO-24H, VPO-48H, VPO-72H and VPO-96H catalysts showed the similar XRD diffraction patterns composed of a well-crystallized $(VO)_2P_2O_7$ phase. The catalysts were characterized by three main peaks appeared at 2θ = 22.9 °, 28.4 °, 29.9 ° correspond to (020), (204) and (221), respectively as shown in Figure 1.

However, a very insignificant peak found at 2θ = 21.5 ° was observed for all the catalyst samples, which corresponds to β-$VOPO_4$ phase. This extra peak was shown to be more prominent as the second-stage reflux duration increased from 24 h to 72 h. The peak was then lowered for the VPO-96H. This indicates that longer second-stage reflux duration of sesquihydrate precursor will induce the formation of V^{5+} phase component in the catalyst until the duration of 72 h.

The peak at 2θ = 22.9 ° which is assigned to reflection plane (020) was found to be more intense and narrower as the second-stage reflux duration increased from 24 h to 96 h. However, the intensity of the (204) reflection plane (2θ = 28.4 °) increased from 24 h to72 h, then dropped slightly at 96 h.

The crystallite size is given by Debye-Scherrer equation:

$$t = \frac{0.89\lambda}{\beta_{hkl} \cos \theta_{hkl}}$$

where t is the crystallite size for (h k l) phase, λ is the X-ray wavelength of radiation for CuK_α, β_{hkl} is the full-width at half maximum (FWHM) at (h k l) peak and θ_{hkl} is the diffraction angle for (h k l) phase.

The FWHM of the (020) and (204) planes are used to determine the crystallite size of the catalysts. The line width increases with the decreasing size of the crystallites. The change in the FWHM of the (020) reflection is directly proportional to the change in the thickness of the particles in the (100) direction. Hence, it has been proposed by some researchers that the oxidation of $(VO)_2P_2O_7$ catalyst normally starts at the side faces of the (100) plane.

From the results, the VPO-48H catalyst had shown the highest FWHM (1.7077°), which means it has smallest crystallite size (46.91Å). It was then followed by VPO-96H, with FWHM = 1.5077° and its crystallite size for the (020) plane is 53.14 Å. Subsequently, the crystallite sizes for the (020) plane of VPO-72H and VPO-24H are 57.77Å and 59.45Å, respectively as shown in Table 1.

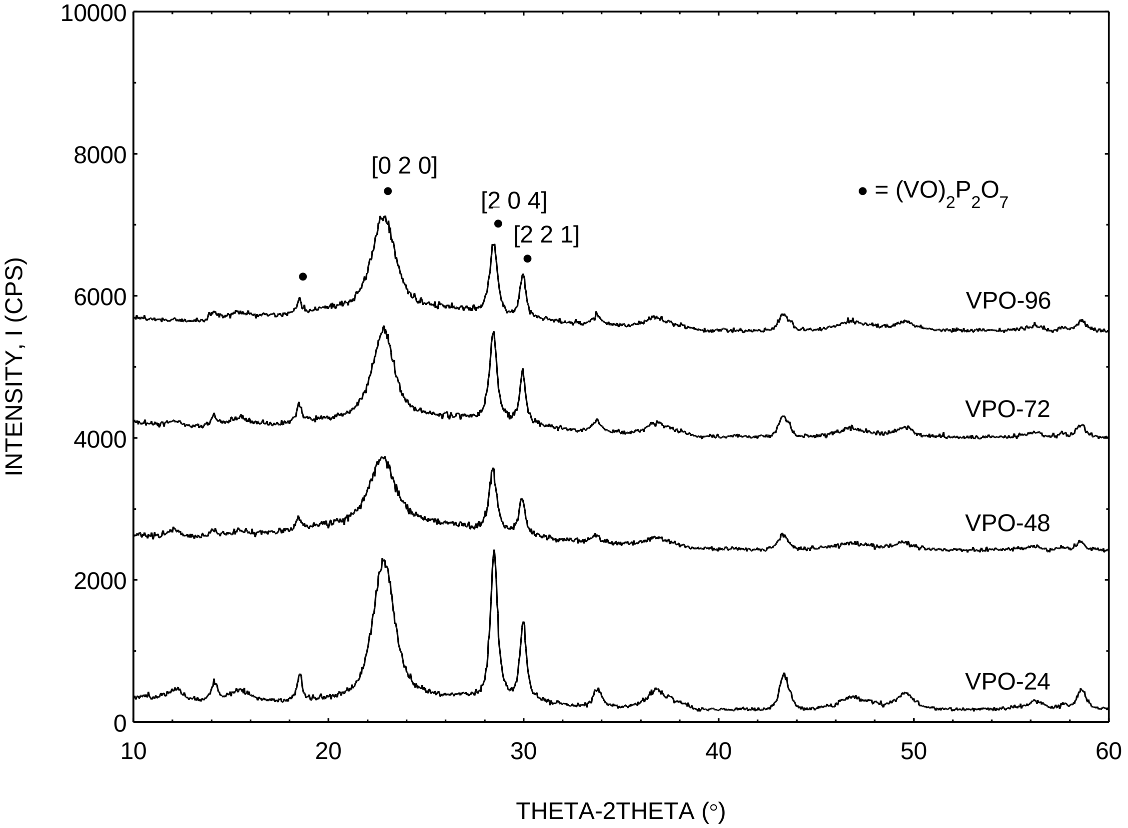

Figure 4.0: XRD patterns of VPO-24H, VPO-48H, VPO-72H and VPO-96H catalysts.

Table 4.0

XRD data of VPO catalysts for different second-stage reflux duration.

Catalyst	FWHM (°)			Crystallite Size (020) (Å)	Crystallite Size (204) (Å)	Crystallite Size (221) (Å)
	(020)	(204)	(221)			
VPO-24H	1.3478	0.6883	0.6864	59.45	117.73	118.43
VPO-48H	1.7077	0.6896	0.6503	46.91	117.42	124.98
VPO-72H	1.3866	0.6426	0.6180	57.77	126.01	131.48
VPO-96H	1.5077	0.6844	0.6400	53.14	118.32	127.01

4.2 Brunauer-Emmer-Teller (BET) Surface Area Measurements

The surface areas of the VPO catalysts that were prepared with different duration of second-stage reflux are as follows: 6.765677 m^2/g for VPO-24H, 6.467425 m^2/g for VPO-48H, 9.750987 m^2/g for VPO-72H and 7.668525 m^2/g for VPO-96H (Table 2). From the results obtained, VPO-72H had shown the highest specific surface area.

Table 4.1

Specific surface areas of VPO catalysts for different second-stage reflux duration.

Catalyst	Specific BET Surface Area (m^2/g)
VPO-24H	6.77
VPO-48H	6.47
VPO-74H	9.75
VPO-96H	7.67

4.3 EDX, ICP-OES Analyses and Redox Titration

Chemical analyses using ICP-OES indicated that all catalysts with different duration of second-stage reflux consisted of very high phosphorus content due to high P/V atomic ratio. The P/V atomic ratios for all the catalyst samples obtained are: 1.30, 1.47, 1.68 and 1.53 for VPO-24H, VPO-48H, VPO-72H and VPO-96H, respectively. As for EDX analyses, the results showed that the P/V atomic ratios were in between 1.16 and 1.40. It was considered slightly deviated from the most compromised range of P/V atomic ratio which gives high catalytic performance.

Guliants *et al.*, 2005 had reported that the optimal catalyst composition is characterized by slight excess of phosphate with respect to the empirical formula of $VOHPO_4 \cdot 1.5H_2O$ precursor. A considerable excess of phosphorus helps stabilize the V^{4+} oxidation state and prevent the over-oxidation of $(VO)_2P_2O_7$ to $VOPO_4$ in air. Hence, Cavani et al. stated that P/V ratio is one of the key factors in catalyst synthesis to prevent $(VO)_2P_2O_7$ and the intermediate amorphous phase from being oxidized to a V^{5+} phosphate.

However, in catalysts with a slight phosphate deficiency (P/V=0.95), the rates of V^{4+} oxidation and reduction are high. The increased V^{5+} content leads to more active but less selective catalysts, but high content of V^{4+} in VPO catalysts results in low catalytic activity. Therefore, Gabassi et al. suggests that the generally acceptable range of P/V atomic ratio for achieving high catalytic performance is from 1.05 to 1.10.

For the redox titration, the average oxidation numbers of the vanadium and percentage of V^{5+} and V^{4+} oxidation states are also summarized in the Table 2. The results showed that there is only slight variation among the average oxidation numbers obtained. It had increased from 4.1593 for VPO-24H to 4.2326 for VPO-48H and 4.2524 for VPO-72H, but dropped to 4.2367 for VPO-96H.

The results are compromised with the XRD results, which showed that VPO-72H had the largest crystallite sizes for the (204) and (221) planes and second-largest size for the (020) that were contributed by the oxidation of V^{4+} phase into V^{5+} phase. It was followed by VPO-96H, VPO-48H and VPO-24H had shown the smallest crystallite size of 59.45Å, 117.73Å and 118.43Å for (020), (204) and (221) planes. The existence of V^{5+} phase in the catalysts had also been proven by the very weak peaks observed at $2\theta = 21.5°$, which belong to β-$VOPO_4$ (type of V^{5+} phases).

Table 4.2

Chemical compositions, average oxidation numbers and percentages of V^{4+} and V^{5+} oxidation states present in the VPO catalysts for different duration of second-stage reflux.

Catalyst	P/V Atomic Ratio		V^{4+} (%)	V^{5+} (%)	Average Oxidation Number
	ICP	EDX			
VPO-24H	1.30	1.16	1.90	0.36	4.1593
VPO-48H	1.47	1.18	1.45	0.44	4.2326
VPO-72H	1.68	1.40	1.54	0.52	4.2524
VPO-96H	1.53	1.28	1.58	0.49	4.2367

4.4 Scanning Electron Microscopy (SEM)

The surface morphologies of the VPO catalysts that are prepared for different second-stage reflux duration retrieved by scanning electron microscopy (SEM) are shown in Fig. 2(a) – (d). These catalyst samples showed the similar principal structures. The structures are consisting of different sizes of plate-like crystals, which were agglomerated into the characteristic of rosebud-shape clusters. These plate-like crystallites are comprised of agglomerates of $(VO)_2P_2O_7$ platelets that expose the (100) crystallite plane. The amount of the platelet in the characteristic rosebud-shape agglomerates was discerned to be different for the series of VPO catalyst.

The VPO catalysts which had been refluxed for 72 h during the second-stage reflux, VPO-72H appeared to have the most prominent and most number of rosebud-shape agglomerates. This explains the highest BET specific area (9.75 m^2/g) shown by VPO-72H although there contained lesser amount of V^{4+} phase. Hence, there appeared to be a trend whereby the agglomerates started to form during 24 h of second-stage reflux, therefore the VPO-24H showed the least clear and less amount of rosebud-shape agglomerates. As the second-stage reflux duration increased to 48 h, the sharper rosebud-shape agglomerates were formed and the $(VO)_2P_2O_7$ platelets are shown more clearly. However, as the reflux duration increased to 96 h, the rosebud-shape agglomerates in the VPO-96H were disturbed, some $(VO)_2P_2O_7$ platelets were destroyed during calcination. This caused the specific surface area to be lowered to 7.76 m^2/g.

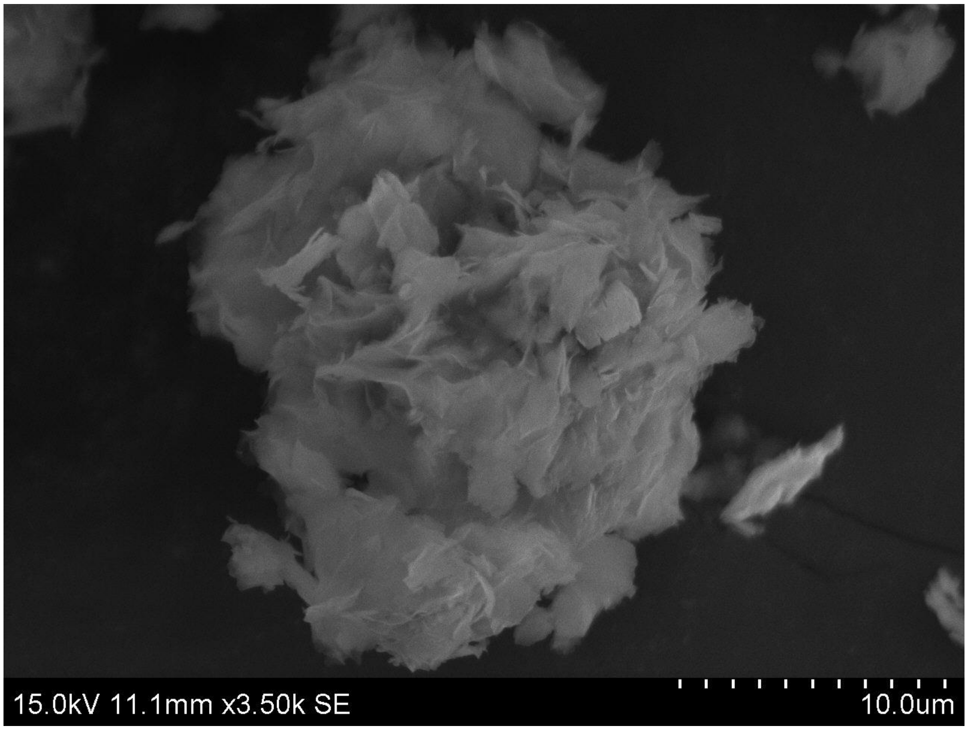

(a)

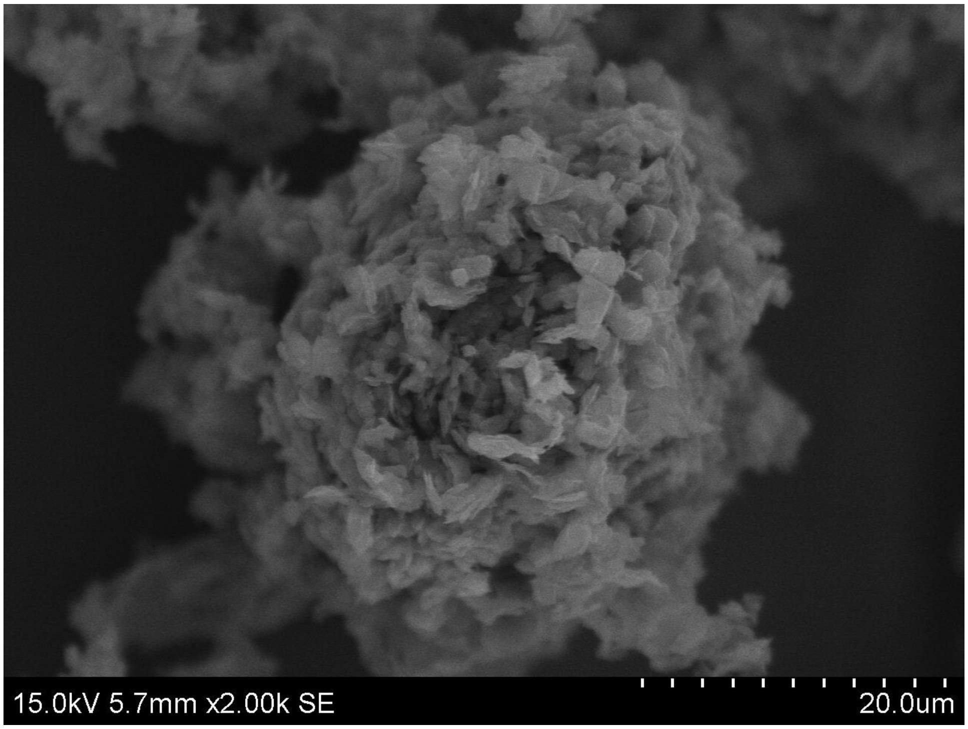

(b)

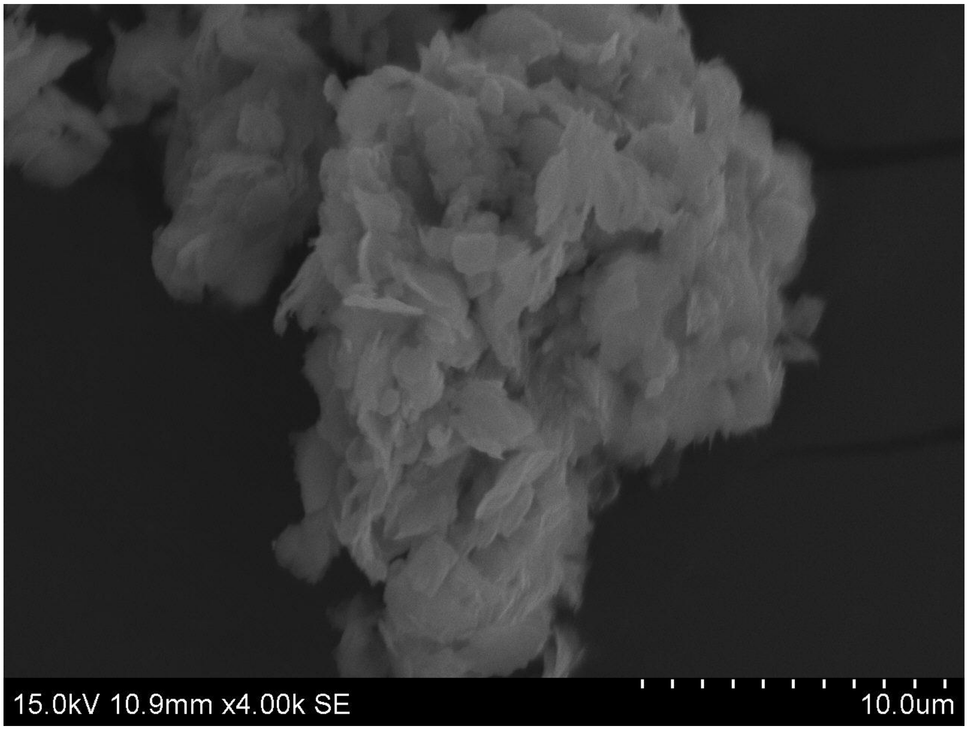

(c)

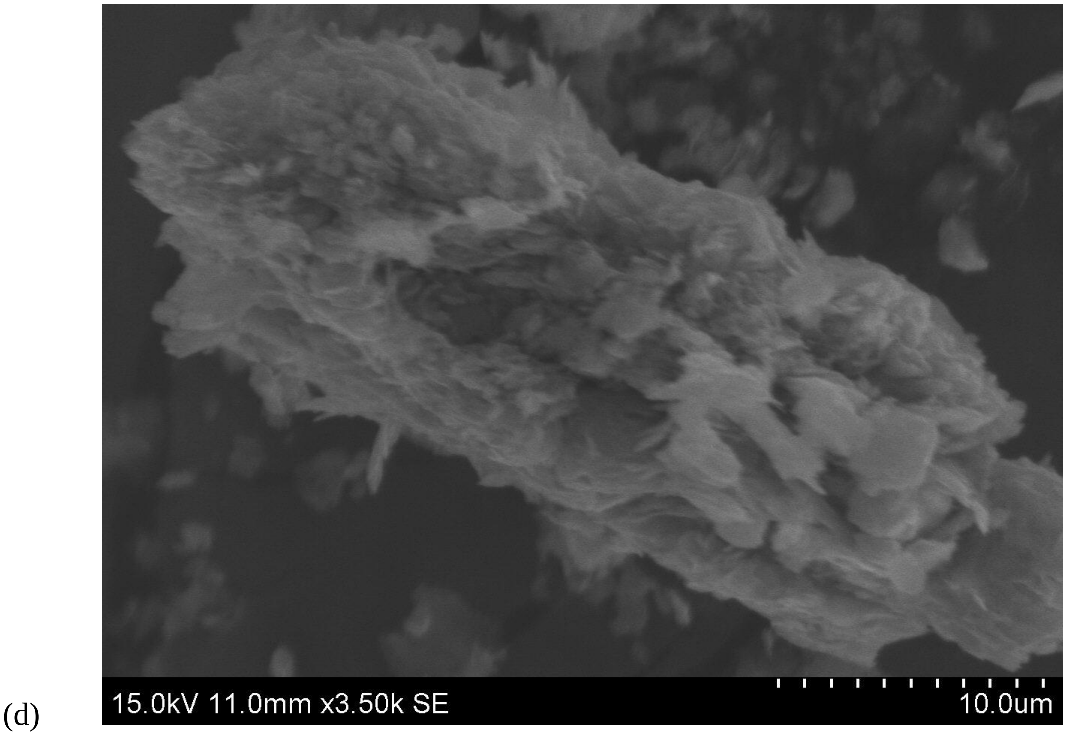

Figure 4.1: SEM micrographs of (a) VPO-24H, (b) VPO-48H, (c) VPO-72H, (d) VPO-96H

CONCLUSIONS

Increasing the duration of second-stage reflux for the VPO catalysts, the specific surface area is increased also until the optimal duration of 72 h which showed the highest specific surface area (9.75m^2/g). This means that VPO-72H has the highest activity among the catalyst samples analyzed.

However, VPO-72H catalyst has also the highest content of V^{5+} phase, which was shown by the high percentage of V^{5+} (25.24%) in the redox titration results. This was further proven by the ICP and EDX results which showed the highest P/V atomic ratio (ICP: 1.68 and EDX: 1.40) for VPO-72H catalyst as high P/V ratio will increase the oxidation rate of V^{4+} phase into V^{5+} phase. High content of V^{5+} will led to high selectivity of the catalysts which means VPO-72H catalyst has both high activity and selectivity. Hence, the VPO-72H catalyst synthesized via sesquihydrate route gives the optimal catalytic performance.

Subsequently, it was followed by VPO-96H catalyst which showed the second-highest specific surface area (7.67m^2/g) and P/V atomic ratio (ICP: 1.53 and EDX: 1.28). From the results of the analyses, the trend is significant that the catalytic performance increased from the second-stage reflux duration of 24 h until the optimal 72 h. The catalytic performance deteriorated when the length of time of the second-stage reflux exceed 72 h. Besides, all catalyst samples exhibited good crystalline with characteristic peaks of $(VO)_2P_2O_7$ phase and their surface morphologies were to found be similar which were in rosebud-shape agglomerates.

REFERENCES

B. Viswanathan *et al.* (2002). Catalysis: Principles and Applications. Narosa Publishing House Pvt. Ltd.

C.H. Bartholomew and R.J. Farrauto (2005). Fundamentals of Industrial Catalytic Processes (2nd Ed.). Wiley-Interscience, A John Wiley & Sons Inc.

G.C. Chitanu *et al.* (2005). Synthesis and Characterization of Maleic Anhydride Copolymers and Their Derivatives. *Revue Roumaine de Chimie*, 2006: 51(9), 923-929.

H.S. Fogler (2008). Elements of Chemical Reaction Engineering (4th Ed.). Pearson, Prentice Hall.

I. Chorkendorff and J.W.Niemantsverdriet (2003). Concepts of Modern Catalysis and Kinetics. Wiley-Interscience, A John Wiley & Sons Inc.

J.B. Benziger *et al.* (1997). New Precursors to VPO Catalysts. Catalysis Today: 33 (1997) 49-56

L. Cornaglia *et al.* (2003). The Beneficial Effect of Cobalt on VPO Catalysts. Catalysis Today: 78 (2003) 291-301

L. Griesel *et al.* (2004). Preparation of Vanadium Phosphate Catalysts from $VOPO_4 \cdot 2H_2O$: Effect of $VOPO_4 \cdot 2H_2O$ Preparation on Catalyst Performance. Journal of Molecular Catalysis A: Chemical 220 (2004) 113-119

L.K. Leong *et al.* (2010). The Effect of Bi Promoter on Vanadium Phosphate Catalysts Synthesized via Sesquihydrate Route. Catalysis Today (2010).

N. Govender *et al.* (2004). Controlling Factors in the Selective Conversion of *n*-Butane over Promoted VPO Catalysts at Low Temperature. Catalysis Today: 97 (2004) 315-324

S. Ieda *et al.* (2005). Involvement of Active Sites of Promoted Vanadyl Pyrophosphate in Selective Oxidation of Propane. Journal of Catalysis: 236 (2005) 304-312

T.R. Felthouse et al. (2001). Maleic Anhydride, Maleic Acid and Fumaric Acid. Huntsman Petrochemical Corp. Austin Laboratories, Austin, Texas, USA

V.V. Guliants *et al.* (1995). Evolution of the Active Surface of Vanadyl Pyrophosphate Catalysts. Catalysis Letter: 32 (1995) 379-386

V.V. Guliants (1999). Structure-Reactivity Relationships in Oxidation of C4 Hydrocarbons on Supported Vanadia Catalysts. Catalysis Today: 51 (1999) 255-268

V.V. Guliants *et al.* (1999). The Oxidation of C_4 Molecules on Vanadyl Pyrophosphate Catalysts. Studied in Surface Science and Catalysis, Vol. 101

V.V. Guliants and M.A. Carreon (2005). Vanadium-Phosphorus-Oxide: from Fundamentals of *n*-Butane Oxidation to Synthesis of New Phases. Catalysis, Vol. 18, The Royal Society of Chemistry, 2005.

W. Nie *et al.* (2002). Comparative Studies on the VPO Specimen Supported on Mesoporous Al-containing MCM-41 and Large-pore Silica. Applied Catalysis A: General 244 (2003) 265-272

Xue and Zhi-yang (Allen) (1999). In-situ Vibrational Spectroscopic Investigation of C_4 Hydrocarbon Selective Oxidation over Vanadium Phosphorus Oxide. Iowa State University.

Y.H. Taufiq-Yap *et al.* (2008). Effect of Different Calcination Environments on the Vanadium Phosphate Catalysts for Selective Oxidation of Propane and *n*-Butane. Catalysis Today: 131 (2008) 285-291

Y.H. Taufiq-Yap *et al.* (2001). The Effect of the Duration of *n*-Butane / Air Pretreatment on the Morphology and Reactivity of $(VO)_2P_2O_7$ Catalysts. Catalysis Letters: Vol. 74, No. 1-2, 2001.

Y.H. Taufiq-Yap and K.C. Waugh (2003). The Effect of Varying the Duration of the Butane / Air Pretreatment on the Morphology and Reactivity of $(VO)_2P_2O_7$ Catalysts. Catalysis Today: 81 (2003) 215-225

Y.H. Taufiq-Yap *et al.* (2006). Promotional Effect of Bismuth as Dopant in Bi-Doped Vanadyl Pyrophosphate Catalysts for Selective Oxidation of *n*-Butane to Maleic Anhydride. Journal of Natural Gas Chemistry: 15 (2006) 297-302

Y.H. Taufiq-Yap *et al.* (2004). Synthesis and Characterization of Vanadyl Pyrophosphate Catalysts via Vanadyl Hydrogen Phosphate Sesquihydrate Precursor. Catalysis Today: 93-95 (2004) 715-722

APPENDICES

Appendix A

Volume of Isobutanol Used

Molecular formula of vanadyl phosphate dihydrate = $VOPO_4 \cdot 2H_2O$

Molecular weight of Vanadium = 50.9414 g/mol

Molecular weight of Phosphate = 30.97376 g/mol

Molecular weight of Oxygen = 15.9994 g/mol

Molecular weight of Hydrogen = 1.0079 g/mol

Molecular weight of $VOPO_4 \cdot 2H_2O$ = 50.9414 g/mol + (7×15.9994 g/mol) + 30.97376 g/mol + (4×1.0079 g/mol)

= 197.94256 g/mol

No. of mol of $VOPO_4 \cdot 2H_2O$ $= \frac{mass}{molecular\ \ weight}$

$= \frac{10\ g}{197.94256\ g/mol}$

= 0.05052 mol

(50 mol alcohol/ mol $VOPO_4 \cdot 2H_2O$)

For 1 mol of $VOPO_4 \cdot 2H_2O$, 50 mol of alcohol (iso-butanol) is needed.

From the calculation as shown above, 0.05052 mol of $VOPO_4 \cdot {}_2H_2O$ is used.

$$\frac{0.05052\,mol\ \mathrm{VOPO4\cdot 2H2O}}{1\,mol\ \mathrm{VOPO4\cdot 2H2O}} \times 50\,mol\ alcohol = 2.5260\,mol\ alcohol$$

Thus, 2.5260 mol of alcohol (iso-butanol) is needed for 0.05052 mol of $VOPO_4 \cdot {}_2H_2O$.

Molecular formula of iso-butanol = $C_4H_{10}O$

Molecular weight of Carbon = 12.011 g/mol

Molecular weight of Oxygen = 15.9994 g/mol

Molecular weight of Hydrogen = 1.0079 g/mol

Molecular weight of $C_4H_{10}O$ = (4×12.011 g/mol) + (10×1.0079 g/mol)

+ 15.9994 g/mol

= 74.1224 g/mol

Density of $C_4H_{10}O$ = 0.802 g/cm^3 at 20 ℃

Mass of $C_4H_{10}O$ = 74.1224 g/mol × 2.5260 mol

= 187.2332 g

Density $= \frac{mass}{volume}$

Volume of iso-butanol $= \frac{mass}{density}$

$= \frac{187.2332\ g}{0.802\ g/cm^3}$

= 233.4578 cm^3

Therefore, total volume of iso-butanol added is 233.4578 cm^3.

Appendix B

Volume of Distilled Water Used

(24 ml H_2O/ g solid)

15 g of V_2O_5 is used as a starting material.

Thus, the volume of distilled water needed = 15 g × (24 ml H_2O/ g solid)

= 360 ml

Appendix C

Crystallite Size Measurements by using Powder XRD Technique

Crystallite size, T given by Debye-Scherrer equation: $T(\text{Å}) = \frac{0.89\lambda}{FWHM \times cos\theta}$

$$\text{Given } \lambda_{\text{Cu K}\alpha} = 1.54\text{Å}$$

$$\text{FWHM (rad)} = \text{FWHM }(°) \times \frac{\pi}{180°}$$

Appendix D

Preparation of Diphenylamine, Ph_2NH Indicator (Redox Titration)

1 g of diphenylamine was weighed and dissolved in a few ml of concentrated sulphuric acid, H_2SO_4. Then the solution was transferred to a 100 ml volumetric flask and further top up with concentrated H_2SO_4.

Appendix E

Preparation of 2 M Sulphuric Acid, H_2SO_4 Solution

Concentrated H_2SO_4 (95- 98%)

1L = 1.84 kg = 1840 g/ 1000cm^3 = 1.84 g/cm^3

Molecular weight of H_2SO_4 = 2(1.00 g/mol) + 32.07 g/mol + 4(16.00 g/mol)

= 98.07 g/mol

Concentration of 95- 98% H_2SO_4 $= \frac{1.84\ g/cm^3}{98.07\ g/mol} \times \frac{95}{100} \times 1000 = 17.82\ M$

$M_1V_1 = M_2V_2$ where M_1 = concentration of 95- 98% H_2SO_4

M_2 = concentration of diluted H_2SO_4 (2 M)

V_1 = volume of 95- 98% H_2SO_4

V_2 = volume of diluted H_2SO_4 (2 M)

(17.82 M) (V_1) = (2 M) (1000 cm^3)

V_1 = 112.23 cm^3

Appendix F

Preparation of 0.1 M Sulphuric Acid, H_2SO_4 Solution

$M_1V_1 = M_2V_2$ where M_1 = concentration of 95- 98% H_2SO_4

M_2 = concentration of diluted H_2SO_4 (0.1 M)

V_1 = volume of 95- 98% H_2SO_4

V_2 = volume of diluted H_2SO_4 (0.1 M)

$$(17.82\ \text{M})\ (V_1) = (0.1\ \text{M})\ (1000\ \text{cm}^3)$$

$$V_1 = 5.61\ \text{cm}^3$$

Appendix G

Preparation of 0.01 N Potassium Permanganate, $KMnO_4$ (Redox Titration)

Normality, N (eq/L) = M (mol/L) x *n* (eq/mol)

$MnO^{4-} + 8\ H^{+} + 5\ e^{-} \leftrightarrow Mn^{2+} + 4\ H_2O$

$$\text{Molarity, M (mol/L)} = \frac{N(eq/L)}{n(eq/mol)}$$

$$= \frac{0.01}{5}$$

$$= 0.002\ \text{M}$$

Molecular weight for $KMnO_4$= 39.10 g/mol + 54.94 g/mol + 4 (16.00 g/mol)

= 158.04 g/mol

Weight for $KMnO_4$ in 1000 cm^3 diluted (0.1 M) H_2SO_4 = 0.002 x 158.04

= 0.3161 g

Appendix H

Preparation of 0.01 N Ammonium Iron(II) Sulphate, $(NH_4)_2Fe(SO_4)_2 \cdot 6H_2O$ (Redox Titration)

Normality, N (eq/L) = M (mol/L) x *n* (eq/mol)

$Fe^{2+} + e^- \leftrightarrow Fe^{3+}$

$$\text{Molarity, M (mol/L)} = \frac{N(eq/L)}{n(eq/mol)}$$

$$= \frac{0.01}{1}$$

$$= 0.01\ \text{M}$$

Molecular weight for $(NH_4)_2Fe(SO_4)_2 \cdot 6H_2O$ = 2 (14.00 g/mol) + 20 (1.00 g/mol)

+ 55.85 g/mol + 2 (32.07 g/mol) +

14 (16.00 g/mol)

= 391.99 g/mol

Weight for $(NH_4)_2Fe(SO_4)_2 \cdot 6H_2O$ in 1000 cm^3 diluted (0.1 M) H_2SO_4

= 0.01 x 392.14

= 3.9214 g

Appendix I

Oxidation State of Vanadium (Redox Titration)

Catalysts	V_{AV}	% of V^{4+}	% of V^{5+}
VPO-24H	4.1593	84.07	15.93
VPO-48H	4.2326	76.74	23.26
VPO-72H	4.2524	74.76	25.24
VPO-96H	4.2367	76.33	23.67

According to Niwa and Murakami (1982),

$$T_1 = V^{4+} + 2V^{3+} = 20\,[MnO_4^-]\,V_1 \qquad (1)$$

$$T_2 = V^{5+} + V^{4+} + V^{3+} = 20\,[Fe^{2+}]\,V_2 \qquad (2)$$

$$T_3 = V^{5+} = 20\,[Fe^{2+}]\,V_3 \qquad (3)$$

(2) – (3): $$V^{3+} + V^{4+} = 20\,[Fe^{2+}]\,V_2 - 20\,[Fe^{2+}]\,V_3 \qquad (4)$$

(1) – (4): $$V^{3+} = 20\,[MnO_4^-]\,V_1 - 20\,[Fe^{2+}]\,V_2 + 20\,[Fe^{2+}]\,V_3 \qquad (5)$$

Substitute (5) into (1):

$$V^{4+} + 2(20\,[MnO_4^-]\,V_1 - 20\,[Fe^{2+}]\,V_2 + 20\,[Fe^{2+}]\,V_3) = 20\,[MnO_4^-]\,V_1$$

$$V^{4+} = 20\,[MnO_4^-]\,V_1 - 40\,[MnO_4^-]\,V_1 + 40\,[Fe^{2+}]\,V_2 - 40\,[Fe^{2+}]\,V_3$$

$$= 40\,[Fe^{2+}]\,V_2 - 40\,[Fe^{2+}]\,V_3 - 20\,[MnO_4^-]\,V_1 \qquad (6)$$

Substitute (5) and (6) into (2):

$20\,[Fe^{2+}]\,V_2 = V^{5+} + (40\,[Fe^{2+}]\,V_2 - 40\,[Fe^{2+}]\,V_3 - 20\,[MnO_4^-]\,V_1) + (20\,[MnO_4^-]\,V_1 - 20\,[Fe^{2+}]\,V_2 + 20\,[Fe^{2+}]\,V_3)$

$$V^{5+} = 20\,[Fe^{2+}]\,V_3 \qquad (7)$$

From (5): $V^{3+} = 20\,(0.01)\,V_1 - 20\,(0.01)\,V_2 + 20\,(0.01)\,V_3$

$$= 0.2\,(V_1 - V_2 + V_3) \qquad (8)$$

From (6): $V^{4+} = 40\,(0.01)\,V_2 - 40\,(0.01)\,V_3 - 20\,(0.01)\,V_1$

$$= 0.4\,V_2 - 0.4\,V_3 - 0.2\,V_1 \qquad (9)$$

From (7): $V^{5+} = 20\,(0.01)\,V_3$

$$= 0.2\,V_3 \qquad (10)$$

The average vanadium valence is calculated as:

$$V_{AV} = \frac{3V^{3+} + 4V^{4+} + 5V^{5+}}{V^{3+} + V^{4+} + V^{5+}} \qquad (11)$$

VPO-24H

$V_1 = 10.10$, $V_2 = 11.60$, $V_3 = 1.80$

From (6): V^{4+} $= 40\ (0.01)\ V_2 - 40\ (0.01)\ V_3 - 20\ (0.01)\ V_1$

$= 0.4\ V_2 – 0.4\ V_3 – 0.2\ V_1$

$= 0.4\ (11.60) – 0.4\ (1.80) – 0.2\ (10.10)$

$= 1.9$

From (7): V^{5+} $= 20\ (0.01)\ V_3$

$= 0.2\ V_3$

$= 0.2\ (1.80)$

$= 0.36$

The average vanadium valence is calculated as:

$$V_{AV} = \frac{3V^{3+} + 4V^{4+} + 5V^{5+}}{V^{3+} + V^{4+} + V^{5+}}$$

$$= \frac{3(0) + 4(1.90) + 5(0.36)}{1.9 + 0.36}$$

$= 4.1593$

If V_{AV} of VPO-24H = 4.1593

V^{5+} (%) = 15.93 %

V^{4+} (%) = (100 – 15.93) %

= 84.07 %

VPO-48H

$V_1 = 8.60$, $V_2 = 10.05$, $V_3 = 2.20$

From (6): $V^{4+} = 40\ (0.01)\ V_2 - 40\ (0.01)\ V_3 - 20\ (0.01)\ V_1$

$= 0.4\ V_2 – 0.4\ V_3 – 0.2\ V_1$

$= 0.4\ (10.05) – 0.4\ (2.20) – 0.2\ (8.60)$

$= 1.42$

From (7): $V^{5+} = 20\ (0.01)\ V_3$

$= 0.2\ V_3$

$= 0.2\ (2.20)$

$= 0.44$

The average vanadium valence is calculated as:

$$V_{AV} = \frac{3V^{3+} + 4V^{4+} + 5V^{5+}}{V^{3+} + V^{4+} + V^{5+}}$$

$$= \frac{3(0) + 4(1.42) + 5(0.44)}{1.42 + 0.44}$$

$= 4.2366$

If V_{AV} of VPO-48H = 4.2366

V^{5+} (%) = 23.66 %

V^{4+} (%) = (100 – 23.66) %

= 76.34 %

VPO-72H

$V_1 = 7.90$, $V_2 = 10.40$, $V_3 = 2.60$

From (6): V^{4+} $= 40 (0.01) V_2 - 40 (0.01) V_3 - 20 (0.01) V_1$

$= 0.4 V_2 – 0.4 V_3 – 0.2 V_1$

$= 0.4 (10.40) – 0.4 (2.60) – 0.2 (7.20)$

$= 1.54$

From (7): V^{5+} $= 20\ (0.01)\ V_3$

$= 0.2\ V_3$

$= 0.2\ (2.60)$

$= 0.52$

The average vanadium valence is calculated as:

$$V_{AV} = \frac{3V^{3+} + 4V^{4+} + 5V^{5+}}{V^{3+} + V^{4+} + V^{5+}}$$

$$= \frac{3(0) + 4(1.54) + 5(0.52)}{1.54 + 0.52}$$

$= 4.2524$

If V_{AV} of VPO-72H = 4.2524

V^{5+} (%) = 25.24 %

V^{4+} (%) = (100 – 25.24) %

= 74.76 %

VPO-96H

$V_1 = 8.55$, $V_2 = 10.65$, $V_3 = 2.43$

From (6): V^{4+} $= 40\ (0.01)\ V_2 - 40\ (0.01)\ V_3 - 20\ (0.01)\ V_1$

$= 0.4\ V_2 – 0.4\ V_3 – 0.2\ V_1$

= 0.4 (10.65) – 0.4 (2.43) – 0.2 (8.55)

= 1.58

From (7): V^{5+} = 20 (0.01) V_3

= 0.2 V_3

= 0.2 (2.43)

= 0.49

The average vanadium valence is calculated as:

$$V_{AV} = \frac{3V^{3+} + 4V^{4+} + 5V^{5+}}{V^{3+} + V^{4+} + V^{5+}}$$

$$= \frac{3(0) + 4(1.58) + 5(0.49)}{1.58 + 0.49}$$

= 4.2367

If V_{AV} of VPO-96H = 4.2367

V^{5+} (%) = 23.67 %

V^{4+} (%) = (100 – 23.67) %

= 76.33 %